Ship response estimation in early design stage

Xiaochi Cai

Thesis submitted for examination for the degree of Master of Science in Technology.

Espoo 30.5.2016

Thesis supervisor:

Prof. Jani Romanoff (Aalto)

Prof. Anders Rosén (KTH)

Thesis advisor:

D.Sc. (Tech.) Jasmin Jelovica

Aalto University
School of Engineering

Author: Xiaochi Cai

Title: Ship response estimation in early design stage

Date: 30.5.2016 Language: English Number of pages: 8+75

Department of Mechanical Engineering

Professorship: Maritime Engineering

Supervisor: Prof. Jani Romanoff (Aalto) & Prof. Anders Rosén (KTH)

Advisor: D.Sc. (Tech.) Jasmin Jelovica

A practical way to estimate the ship response in early design stage is investigated in this thesis. Focus has been put on the ship vertical bending moment and shear force in operation area. ISSC spectrum is used to indicate the sea state. *Napa strip method* is employed to derive the transfer function. The ship response is thus generated in frequency domain. The vertical bending moment and shear force along the ship are then calculated according to the critical wave case indicated from the response function.

Based on the results, the validation of DNV-GL rule and IACS rule is discussed. In this case, the overestimation is discovered for the still water vertical bending moment and shear force. On the other hand, there is underestimation in wave vertical bending moment and shear force. The dynamic vertical bending moment and shear force is reasonable. Since only static loads and dynamic loads are required in the rules, the rules are judged as valid in the early design stage.

The feasibility of *Napa strip method* has been commented and the *Napa strip method* is judged practical according to its accuracy and time consumption.

For ship design, the wavelength and the wave steepness are the main parameters affecting the loads on hull. The block coefficient is crucial for the nonlinearity in hogging and sagging condition.

More models, especially other types of ships are expected to be analysed for this topic in future study. Other methods, such as *panel method* could take into use in the future work. The probability of operation can be further developed based on this study.

Keywords: preliminary design, NAPA, nonlinearity, strip method, ship response, vertical bending moment, shear force

Preface

I want to thank Professor Jani Romanoff for his good guidance and support in the thesis work. Whenever I had some comfusion, Jani would help me solve the problem and confirm my working track. I also want to present my appreciation to my advisor Jasmin Jelovica, who helped in application and thesis writing. I am also grateful for the guidance and opinions from Professor Anders Rosén.

During the applicaiton process, Tapio Seppälä, from *Napa* company, helped me in the software. I would like to thank him for teaching me.

The last but not the least, I would like to send my gratitude to my parents and all my friends, who stood for me and helped me when I was doing the thesis project.

Otaniemi, 30.5.2016

Xiaochi Cai

Contents

Symbols and abbreviations

Physical constants

g gravitational constant $[m/s^2]$, $g = 9.81 m/s^2$
ρ density of sea water $[kg/m^3]$, $\rho = 1025\ kg/m^3$

Nomenclature

A_{ij}	added water mass $[kg]$ or added water mass moment of inertia $[kgm^2]$, $i\&j$ different degrees of freedom
A_s	area of the cross section in Lewis confromal mapping
a_{2n-1}	conformal mapping coefficients $(n = 1, ...N)$, $a_{-1} = 1$
B	ship breath $[m]$
B_{ij}	damping coefficient, translative $[kg/s]$, rotative $[kgm^2/s]$, $i\&j$ different degrees of freedom
B_s	sectional breath on the water line in Lewis conformal mapping
C	wave coefficient in IACS rule
C_{ij}	hydrostatic coefficient, translative $[kg/s^2]$, rotative $[kgm^2/s^2]$, $i\&j$ different degrees of freedom
C_B	block coefficient
C_W	wave coefficient in DNV-GL rule
c	wave propagation speed, also phase velocity $[m/s]$
D_s	sectional draught in Lewis conformal mapping
F_1, F_2	distribution factor along the ship length of wave vertical shear force, for positive and negative conditions, ruled by IACS
F_i^{sw}	force or moment related to ship motions in calm water
F_i^{wm}	force or moment related to the motion of wave, excitation force, excitation moment
Fn	Froude number, $Fn = V/\sqrt{gL}$
$F_W(+)$, $F_W(-)$	wave vertical shear force $[kN]$, ruled by IACS
F_{W2}, F_{W7}	wave vertical shear force at $x = 0.25L$ and $x = 0.7L$, ruled by IACS
f	force $[kN]$ or moment $[kNm]$
f_p	strength assessment coefficient related to the service area, ruled by DNV-GL
f_{q-pos}, f_{q-neg}	distribution factor along the ship for wave vertical shear force, defined by DNV-GL
f_{qs}	distribution factor along the ship for still water vertical shear force, defined by DNV-GL
f_m	distribution factor for wave vertical bending moment along the ship's length, ruled by DNV-GL

f_{nl-vh}, f_{nl-vs}	coefficient considering nonlinear effects ruled by IACS
f_{SW}	distribution factor for still water vertical bending moment along the ship length, ruled by DNV-GL
H	wave height $[m]$
$H_{1/3}$	significant wave height $[m]$
H_z	mean wave height $[m]$
k	wavenumber $[m^{-1}]$
L	ship length $[m]$, accoring to $S2$, is the length at water line
L_{pp}	perpendicular ship length $[m]$
M	distribution factor for wave bending moment ruled by IACS
$M_{dy-h-mid}$, $M_{dy-s-mid}$	ruled dynamic vertical bending moment for hogging and sagging in the middle of the ship
M_s	scale factor of conformal mapping
M_{ij}	water mass $[kg]$ or water mass moment of inertia $[kgm^2]$, $i\&j$ different degrees of freedom
M_{sw}	still water vertical bending moment $[kNm]$
$M_{SW-h-min}$, $M_{SW-s-min}$	maximum allowed still water vertical bending moment $[kNm]$, for hogging and sagging
M_{SW-min}	absolute maximum of $M_{SW-h-min}$ and $M_{SW-s-min}$ with $f_{SW} = 1.0$
M_v	vertical bending moment $[kNm]$
M_{wv}	wave vertical bending moment $[kNm]$
M_{WV-h}, M_{WV-s}	wave vertical bending moment $[kNm]$ ruled by DNV-GL, for hogging and sagging
$M_{WV-h-min}$, $M_{WV-s-min}$	maximum allowed wave vertical bending moment $[kNm]$, for hogging and sagging
p	pressure $[Pa]$
Q_{sw}	still water vertical shear force $[kN]$
Q_{WV-pos},Q_{WV-neg}	wave shear force $[kN]$, in positive and negative condition, ruled by DNV-GL
$Q_{SW-pos-min}$,$Q_{SW-neg-min}$	still water shear force in seagoing condition $[kN]$, for hogging and sagging, ruled by DNV-GL
Q_v	vertical shear force $[kN]$
Q_{wv}	wave vertical shear force $[kN]$
$S_\zeta(\omega)$	wave spectrum
$S_\eta(\omega)$	response spectrum
T	wave period $[s]$
T_z	zero crossing period $[s]$
$U_{19.5}$	mean wind speed at 19.5 meter height above sea level $[m/s]$
V	ship speed $[knot]$
x, y, z	spatial coordinates $[m]$
$Y(\omega)$	transfer function

ϵ, ϵ^η	phase shift; phase shift for wave
ζ	vertical position of wave surface $[m]$
ζ_0	wave amplitude $[m]$
$\hat{\zeta}$	complex wave amplitude
η, $\eta(\zeta)$	ship motion
η_i, $\dot{\eta}_i$, $\ddot{\eta}_i$	ship motions, speeds, accelarations in different degrees of freedom
η_0, η_{i0}	ship motion amplitude
λ	wavelength $[m]$
ϕ	velocity potential
μ	wave direction $[^o]$, $\mu = 0$ following sea, $\mu = 180^o$ head sea
σ_s	sectional area coefficient in Lewis conformal mapping
σ_η^2	variance
σ_η	standard deviation, also known as RMS (Root Mean Square)
ω	angular frequency $[rad/s]$
ω_e	frequency of encounter $[rad/s]$
ω_m	wave modal frequency $[rad/s]$, $\omega_m = 0.4\sqrt{g/H_{1/3}}$

Operators

∇^2	Laplace operator
$\frac{\partial}{\partial t}$	partial derivative with respect to variable t
$\int_a^b dx$	integration with respect to variable x
$\sum_i^N$	sum over index i to N

Abbreviations

BV	Bureau Veritas (France), ship class society
CoG	Center of Gravity
DoF	Degree of Freedom
DNV	Det Norske Veritas (Norway), ship class society
DNV-GL	ship class society, combined by DNV and GL
EoM	Equation of Motions
GL	Germanischer Lloyd (Germany), ship class society
IACS	International Association of Classification Societies
ISSC	International Ships & Offshore Structures Congress
ITTC	International Towing Tank Conference
JOWSWAP	Joint North Sea Wave Project
SSC	Ship Structure Committee
VBM	vertical bending moment
VSF	vertical shear force

1 Intoduction

1.1 Background and motivation

All ships are designed for some certain purposes, such as pleasure, transportation, racing, war, research and rescue. It is preferred that the function of a certain ship is maximally fufilled and most benefits are expected. However, except for those functional designs on ships, other aspects shall be considered to achieve a certain level of the safety since ships are always operating in wind and wind generated waves. For example, a commercial cargo ship is tended to accommodate more cargo. In order to accommodate more cargo, the cargo area is tended to be designed as large as possible. However, more cargo might lead to a higher center of gravity, which decreases the ship's stability property. On the other hand, too large safety margins result in extensive fuel cost and low transportation efficiency. The balance between ship's performance and safety is thus a challenge in ship design.*[1]*

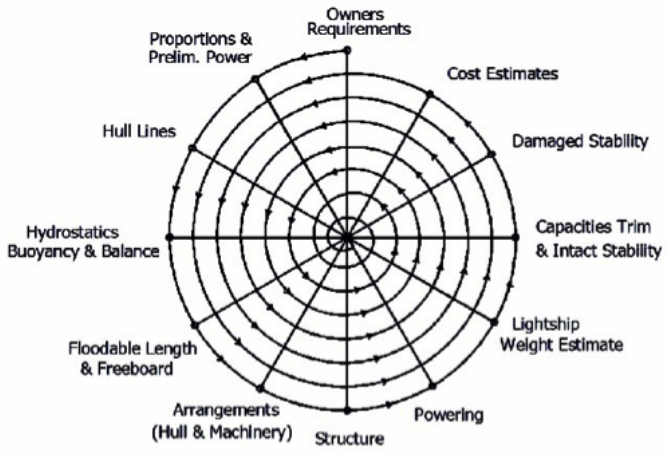

Figure 1: Design process for a commercial ship.*[2]*

Figure 1 indicates the ship design process for a commercial ship. The ship design starts from the owners' requirements. The ship is assigned with some particular task in accordance to the requirements. Based on this, the design circle begins to run round and round until the decisions have taken all aspects into consideration and satisfy a highest transportation effeciency with respect to basic safety requirement.

In ship design, it is essential to estimate the ship behavior and its structrual endurance against waves. A proper design should try to avoid any potential dangers. An example of failure in bending strength can be seen in Figure 2. In this case, the wavelength is about the same as the ship length and the middle section of the ship was pushed up and down by an alternating vertical bending moment. As soon as the actual bending moment created by the loadings and waves appeared to be more than the design capacity of the structure, the hull structure could not afford. The ship was thus broken in the middle.

Therefore, it is quite important to raise an adequate structrual requirement during the early design stage. Regarding the severity of this issue, ship class

Figure 2: Structural failure due to hull bending.*[3]*

societies including all the members of International Association of Classification Societies(IACS) have their own requirements in ruling the structrual strength when designing a ship. The vertical bending moment and shear force must be estimated and reported to be approved before building a ship. In the rules of those class societies, the maximum vertical bending moment and shear force along the ship are limited respectively. The ship should be designed to avoid the response beyond the rule limitation in its serving sea areas.

In general, there are three ways to get a reasonable estimation of ship seakeeping properties including full-scale experiment, model test and computation. A full-scale experiment means to build and test a physical ship model which has the same parameters in size of the real design. For sure, the full-scale experiment would provide accurate prediction. However, to build the full-scale physical model requires large amount of cost in money, time and space or facilities. This method usually is only used when the design object is relatively small and there are lots of uncertainties, but not feasible in a normal commercial ship design. The model test means to build a scaled physical model. Comparing with the full-scale model, it saves much cost, but still, money, time and experimental environment makes it infeasible in the early design stage. The most practical and efficient way is to take the use of computational method. A good simulation is usually accurate enough for the early design stage. The results derived by the computational simulation are also recogonized by various ship class societies for most normal commercial ships.

Nowadays, with the development of computation capacity, numerical calculation has been applied in most fields of study. In ship design industry, lots of commercial softwares have been created to simulate the ship operation and foresee the loads that the ship would face. Each software company has its own selection in the theory generating the ship response in waves. The results derived by different methods behave different in accuracy and computing time. Also each method has its own limitation and the users need to decide which one to use depending on the study case. Usually, the more accurate estimation takes more time in computing. The balance between the accuracy and the feasibility is an inevitable issue that designers should think about. In the early ship design stage, such as the first or second round in the design circle shown in Figure 1, there are lots of unknown details. At this stage, it is

reasonable to leave some less important aspects behind, so as to avoid computing waste of computing time. A practical way to pre-determine the ship response in vertical bending moment and shear force is worth studying.

1.2 State of art

Dealing with the seakeeping problem, there are two commonly used methods to simulate the ship operation in sea states, the *strip method* and the *panel method*. The *strip method* describes the ship with several strip sections along the ship and the hull body is replaced by several cylinders according to the shapes of strip sections. In this manner, the 3D hydrodynamic problem is converted to 2D problem, which makes it much easier in calculating the hydrodynamic force. The hydrodynamic force per unit length of these segments may then be calculated by assuming the cylinder infinitely long. The *panel method* forms the ship in terms of a bunch of flat facets with sinks and sources on the wetted hull surface. The loads on each facet refer to the boundary condition and the ship response is calculated in accordance with automatically derived ship hydrodynamic force which fulfill the boundary condition. The overall hydromechanical forces are thus calculated by the hydrodynamic force on each panels. More details are to be introduced in the later chapters.

Figure 3: Ship slamming on the sea.*[5]*

The two methods are both valid in specific situations. Based on the principle of the methods, various irregular aspects has been noticed and considered during detailed applications, especially when the ship has a forward speed. Those aspects are nonlinearities. For example, as shown in Figure 3, a high-speed craft usually has heavy slamming problem at the fore quarter of the ship, where extra moments should be considered. To ensure the accuracy of simulation, a certain level of nonlinearity shall be considered in the numerical calculation. Figure 4 indicates the composition of wave loads. The nonlinearities actually come from high order items of the solution for hydrostatic and hydrodynamic forces. As pointed by ISSC*[4]*, the nonlinearities can be defined as six levels according to the extent:

– Level 1: Linear

- Level 2: Froude-Krylov nonlinear
- Level 3: Body nonlinear
- Level 4: Body exact (Weak scatter)
- Level 5: Fully nonlinear (Smooth waves)
- Level 6: Fully nonlinear

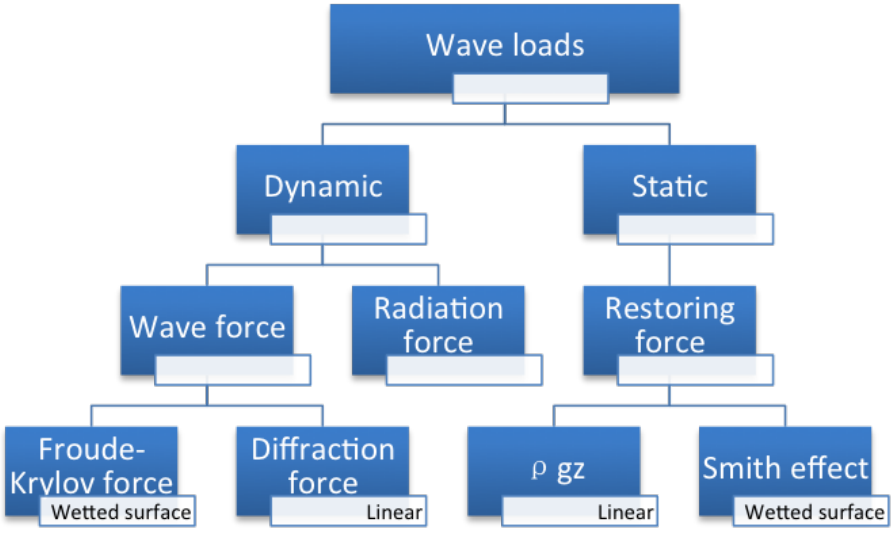

Figure 4: Composition of wave loads.

In Level 1, the water lever is defined as the mean position of the free surface and the wetted body surface is accounted by the mean position of the hull under water. The boundary conditions are applied on the defined water level. For the hydrodynamic problem, only the first order diffraction and radiation solution is concerned. A speed correction is commonly applied in the linear method to avoid computational difficulties. The solution achieves a level of maturity and the problem is practical to solve in the frequency domain. Force and moment magnitudes between the numerically implemented theory and experiments are generally in good agreement for most conditions. However, for the loads on hull girders, the linear method has been pointed out not applicable for the vertical bending moment on container ships by Singh and Sen*[6]*. After comparing the experiment data from the S-175 container ship in regular waves with the calculated results from numerical simulation, they concluded that the linear method gives too low sagging and too large hogging moments.*[4]*

In Level 2, the disturbance potential is calculated the same as linear method, but the hydrostatic pressure over the wetted hull surface is no longer concerned by the mean position of the free surface. The instantaneous position of the hull under the incident wave surface is captured instead. The incident wave forces are evaluated by integrating the incident wave pressure. The Level 2 method is quite common in practical use. Many obvious nonlinearities shall be captured with the cost of little

computing time increasing. The hydrodynamic problem is usually dealt with in the linear frequency domain and transformed to time domain containing the memory effects which offsets the time-independent feature in potential flow theory.*[4]*

In Level 3, the disturbance potential is calculated according to the instantaneous position of the hull under the mean position of the free surface. An indication can be found in Figure 5. The simulation can only be done in time domain. The disturbance potential needs to be calculated for each time step. The time consumption for computation is thus huge comparing with the Level 1 and Level 2 methods.*[4]*

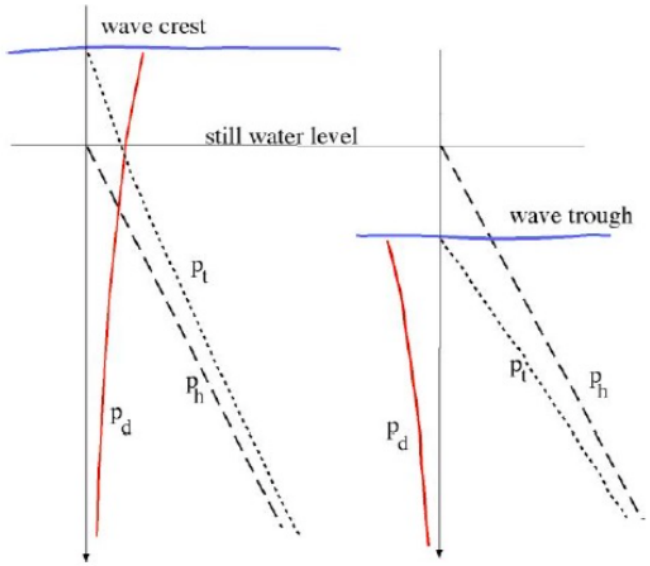

Figure 5: Hydrodynamic force evaluated by the wave height.*[7]*

In Level 4, the methods are similar to Level 3, but the wetted hull surface is defined by the instantaneous position of the hull under the incident wave surface. At this stage, the scattered waves are still assumed to be negligible comparing with the incident waves and the steady waves.*[4]*

In Level 5, the scattered waves are no longer neglected. The impact from them are included in the boundary conditions, but there is no wave breaking or fragmentation of the fluid domain.*[4]*

In Level 6, the methods are regarded fully nonlinear, the breaking and fragmentation shall also be considered. The complexity in Level 6 is huge.*[4]*

The classification in Level 1 suits for either 2D, 2.5D and 3D, while that in Level 2 to Level 5 is best suited for 3D potential theory codes, but strip theory codes will be included. For Level 1 and Level 2 methods, the hydrodynamic problems are mainly solved in frequency domain, while for the other methods, only time domain is applicable. Methods on Level 2 to Level 4 are partially nonlinear methods and given the difficulty in the calculation with Level 5 and Level 6 methods, most commonly used methods are in Level 1 to Level 4. According to the extent of nonlinearity and the differencet between strip method and panel method, the normal applications can

be categorized as 2D linear theory, 2D nonlinear theory, 3D linear theory and 3D nonlinear theory.*[4]*

1.2.1 2D linear theory

In the 20th century, strip method was developed and started to be applied in the ship industry. Since the strip method converts the complex 3D ship motion and hull girder load problems into simplified 2D models, it is quite feasible to apply the 2D linear theory. Of course, the motions simulated with the 2D linear theory has some limitations and inaccuracy, but given the engineering tolerence, it is still widely used in the ship design industry. A basic assumption is that the flow in length direction is negligible. More details of the strip method is introduced in the later chapters.

A classical method to evaluate the loads on hull girder in regular waves is the method raised by Korvin-Kroukovsky*[8]*. The method is based on linear strip theory for heave and pitch motions in head sea wave. Based on this theory, Korvin-Kroukovsky and Jacobs*[9]* did some extension work in validating the theory for ships with low and moderate forward speed. Jacobs*[10]* extended the theory to include the shear force and vertical bending moment in regular head waves. He pointed out the importance of some nonlinear terms such as $Smith\ effect$. However, at that time, some researchers judged the theory of Korvin-Kroukovsky and Jacobs not promising since loads and motions were not derived in a rational mathematical manner but in accordance with "physical intuition".

In the later research from Salvesen et al.*[11]*, Tasai and Takagi*[12]*, and Borodai and Netsvetayev*[13]*, the theory was validated by comparing the mathematically numerical calculated result with experiment data. Their work assures the validation of the theory and provided formulas with more complex manner.

Based on the maturely developed strip theory and Timoshenko beam theory, Bishop et al.*[14][15]* raised a theory concerning the flexibility of ship hull. Pioneer work from Gerritsma and Beukelman*[16]* and Wahab and Vink*[17]* had been cited in Bishop's papers. The work offers the initial thinking of hydroelasticity.

Since the strip method was not able to deal with the vertical hydro turbulence, Newman*[18]* raised a theory of slender body, which extended the strip theory feasible for all the frequency or wave length ranges. Wu, Xia and Du*[19]* extended the theory and made it more general and rational slender-body theory.

Faltinsen and Zhao*[20]* considered the impact of sailing speed and developed a strip method to calculate the seakeeping property and resistance for high-speed vessel. Based on this, Hermundstad, Aarsn and Moan*[21]* and Wu and Moan*[22]* did a generalization work on the theory. Their works presented a more rational hydroelastic formulation of strip theory and analyzed the main factor on structural resonance and the influence from hyroelastic response to structural fatigue.

Besides the research work mentioned before, many other works in developing the 2D linear methods have also been published with various nonlinearity and specific application cases. Most researchers and ship class societies also consider 2D linear theory a feasible and valid way for calculation. The formulas regarding ship motions and structrual strength in rules are mostly based on the theory as well. For example,

in many models, wave bending moment and shear force, the high-order terms are dealt with by converting them into the linear terms, and the principle is still in a linear scale.*[23]*

1.2.2 2D non-linear theory

Nonlinearity includes hydrodynamic nonlinearity and ship structural nonlinearity. The impact from nonlinearity is obvious in the vertical bending moments and shear forces particularly for ships running in severe sea states. Both increasing magnitude and frequency can be obtained in bending moments and shear forces at the fore quarter of most ships, where the linear assumption is violated and the flare angle turns to be V-shape.

Based on a perturbation procedure, Jensen and Pederson*[24]* presented a nonlinear quadratic strip theory in the frequency domain. Both 1st order and 2nd order terms are included in the formulas. The theory takes into account the exciting waves, the flexibility of the ship, the flare of the ship hull geometry, and the perturbation of the two-dimensional hydrodynamic coefficients. It also pointed the differences between hogging and sagging bending moments.

Based on linear strip theory, when calculating the external hydrodynamic force, Yamamoto et al.*[43]* took into consideration the instantaneous sectional immersion by presenting added mass and damping coefficients as a function of time. Slamming force is considered in this nonlinear hytroelasticity method. Similar theories that the motions are calculated in time-domain have been raised by Meyerhoff and Schlachter*[26]*, Fujino and Yoon*[27]*, and Soares*[28]*. However, their theories have a same weakness that the hydrodynamic memory effects are neglected and the hydrodynamic coefficients in Equation of Motions(EoM) are derived for a specific frequency. For irregular waves, the theories are not suitable in use.

Partly nonlinear time-domain strip theory has been developed by Xia, Gu and Wu*[29]*. The theory is extended from 2D potential theory, in which the linear radiation term includes the memory effect by time convolution. The nonlinear slamming force and restoring force are also considered. Ship structure is simulated as Timoshenko beam. The theory has been validated by comparing the simulated results with flexible ship model test.

Söding*[30]*, Bottcher*[31]*, Schlachter*[32]* and Xia J. and Wang Z.*[33]* raised other nonlinear time-domain hydroelasticity theories. The theories introduce the memory effect into higher order terms in EoM and avoid time convolution. The methods reduce the calculation time and are suitable for vertical motion with respect to any frequency. Similar work has been done by Jensen and Dogliani*[34]* and Xia, Wang and Jensen*[35]*.

Now, the 2D nonlinear theories are quite mature given that many nonlinear aspects have been taken into consideration. However, there are still some drawbacks in the theories. The most important factor is the basic assumption of strip method and it is only suitable for slender shape ships. Secondly, all the theories extend the term order from the linear terms to the 2nd order terms. It is still an approximation but has a higher accuracy.

Table 2: Main features of the methods considered by various researchers and ship class societies.*[36]*

Methods	Newcastle	IST1	IST2	DNV	CSSRC	KIT	SRI
Elastic hull	No	No	Yes	No	Yes	Yes	Yes
Non-linear motions	Yes	Yes	No	Yes	Yes	Yes	Yes
Non-linear hydrostatic	Yes	Yes	No	Yes	Yes	Yes	Yes
Non-linear Froude–Krilov	No	Yes	No	Yes	Yes	No	Yes
Non-linear added mass and damping	Yes	No	No	Yes	No	Yes	Yes
Relative motion concept	No	No	Yes	No	No	No	Yes
Smith correction	Yes	No	No	Yes	Yes	Yes	Yes
Linear diffraction exciting forces	No	Yes	No	Yes	No	No	No
Non-linear diffraction exciting forces	No	No	No	Yes	No	No	No
Free surface memory effects	No	Yes	No	No	Yes	No	No
Slamming loads by bottom slamming	No	No	Yes	No	No	Yes	Yes
Slamming loads by momentum slamming	Yes	No	Yes	No	Yes	Yes	Yes
Water on deck	No	Yes	No	Yes	No	No	Yes

As shown in Figure 2, Watanabe*[36]* concludes what the nonlinear features are considered by various researchers and ship class societies. Table 2 presents a comparison of nonlinear time-domain simulation programs from different organizations. In the first column, the nonlinear aspects are listed. The *elastic hull* represents the interaction between the hull and loads. $Non-linear\ motions$ indicates at least one of the force components in the equations of motion to be nonlinear. The *hydrostatic* and $Froude-Krilov$ forces are nonlinear if the wetted surface of the hull takes the water election into consideration and the pressure on the hull shall be calculated given the changing water level. $Non-linear\ added\ mass\ and\ damping$ means that the assumed frequency-dependent sectional coeffcients are dependent of the instantaneous immersion. The *relative motion concept* and $Smith\ effect$ are also related to the changing water level. When diffraction-exciting forces are considered dependent of the instantaneous immersion, they are nonlinear. $Memory\ function$ is a method to include the time influence in the simulation, which is a complement for potential theory. The *slamming loads* are considered when the bottom got slammed by the water loads. The *water on deck* is an aspect for the calculation of motions and structrual loads.*[36]*

The first line in Table 2 shows six organizations who participated in the study, performing the calculations with their own codes. They are University of Newcastle*[37]*, the Technical University of Lisbon (Instituto Superior TeHcnico), (IST1)*[38][39]*, and (IST2)*[40]*, Det Norske Veritas*[41]* (DNV), China Ship Scientific Research Centre*[42]* (CSSRC), Kanazawa Institute of Technology*[43]* (KIT) and the Ship Research Institute of Japan *[44]* (SRI). Except for the DNV method, which is based on panel

method, the other methods are all based on some evaluated strip methods.*[36]*

For an ordinary commercial ship design in the early stage, it usually fits the restrictions from strip method. Given the high applicability and wide recogonization of strip method, this thesis project would take strip method into use. A certain level of nonlinearity should be considered in the application. Details for the level of nonlinearity and the application are introduced in the later chapters. Hereby, another method, panel method, is to be introduced, though it is not applied in this thesis work.

1.2.3 3D linear theory

Although 2D hydrodynamic theories have been proved to be successful in solving some real engineering problems, but there are still some restrictions. Besides the limitation in slender body shape, the 3D hydrodynamic forces at the end quarters are neglected in the 2D hydrodynamic theories. So as to increase the accuracy and expend the solution to a higher accuracy, researchers started to develop 3D theories.

The 3D theory started to get into use when Hess and Smith*[45]* raised idea of panel method. The method utilizes a source distribution on the surface of the body and solves for the distribution necessary to make the normal velocity zero on the boundary. To apply the method, electronic computer is essential since large amount of calculation is required.

Based on the techniques of structural dynamics and hydrodynamics, a general 3D linear hydroelasticity theory has been developed by Wu*[46]*, Price and Wu*[47]* and Bishop et al.*[48]*. Any 3D dry structure dynamic behavior is able to be described by a linear finite element. The interaction between the fluid actions and the distorting wet structure are derived from a 3D theory of potential flow around the flexible floating structure in a seaway.

Aksu, Price and Suhrbier*[47]* extended the theory to time-domain simulation of the behavior of slamming in irregular head and oblique waves. They proved the consistency between the results from 2D and 3D hydroelasticity theories when applying in the slender-shape body and the differences for other shapes.

Du*[50]* provided a complete 3D frequency-domain method. The method retains the linear hydroelasticity theory in the numerical analysis, but also includes the impact of unsteady wave in the boundary condition. The problem is then able to be solved in frequency domain. In the application aspect, researchers such as Lundgren et al.*[51]* applied the theory into various kinds of floating structures. Comparing with slender shape vehicles, the application of panel method has more advantages in estimating the wave response of floating structures.

1.2.4 3D non-linear theory

Wu et al.*[52]* first presented the 3D nonlinear hydroelasticity theory. The expressions of the hydrodynamic forces include the 2nd order term. The nonlinear EoM are presented in either frequency domain or time domain.

Tian and Wu*[53]* studied the impact of nonlinear term for a catamaran in irregular waves. They concluded the prediction in nonlinear shear force and displacement is

20% to 30% larger than the linear model. Besides, comparing with other nonlinear factors, the instantaneous wetted surface is the main reason for nonlinear forces.

1.2.5 Rankine method

Apart from free surface Green's function method, Rankine method is worth mentioning. Rankine method is a simplified Green's function method, that singularities are arranged on both body surface and free surface. It was first raised by Gadd*[54]* and Dawson*[55]*.

Comparing with free surface Green's function method, Rankine method has higher accuracy in calculation but a higher risk in simulation failure. Large amount of computing time is required since the number of cells is over three times more than free surface Green's function.

1.3 Scope of the work

To figure out the vertical bending moment and shear force on hull, there are two basic methods in predicting the ship motions and the loads on hull girders, the *strip method* and the *panel method*. Meanwhile, there are six levels of nonlinearities in the hydrodynamic calculation. All the methods have their own advantages and disadvantages. Accuracy and computational time consumption are the most obvious factors indicating the feasibility of different methods.

In theory, the more accurate the model is, the more reliable results are available. However, the complexity of the methods relates to the accuracy and difficulty of calculation. The difficulty of the methods applied in the production closely relates to the cost. It is wise to avoid unnecessary cost in any engineering industry. Thus, a practical method to predict the ship motions and loads on hull girder is worth studying.

Nowadays, there are a lot of commercial softwares developed and widely used in the ship design. For example, *LaiDyn* is a nonlinear numerical simulation model in time domain. It is capable of evaluating ship motions in regular and irregular seas. However, it is popular for research purposes but not suitable for normal commercial ship design. Among all the softwares, *Napa* occupies a large share in the ship design market and it contains almost all the essential packages for all the early design aspects included in Figure 1. Nowadays, lots of ship models are built in *Napa* before start building. It locates the core competencies on the in-depth understanding of 3D product modelling technologies and naval architectural analyses. The whole design process from the defination of the hull shape, the geometry, the structure and loadings to the calculation in stability, seakeeping and energy comsumption can all be done and reported with *Napa*. The simulation results calculated with *Napa* are always trusted by ship class societies. Given its large market share and highly interated functions, *Napa* is understood to be feasible in predicting the ship motions and loads on hull girder. However, just very little information referring to the study in *Napa* can be found. An exploration in the feasibility of *Napa* for seakeeping calculation is worth carrying on.

It is indicated in the *Napa User Manual[56]*, in the seakeeping module, both strip method and panel method are available In accordance with the six nonlinear levels indicated by ISSC*[4]*, both methods can just achieve the nonlinearity scale of Level 2. Before assigning *Napa* as the tool for the study, a discussion against its value is essential. The features that *Napa* is able to capture is listed as follow:

- Hull shape
- Weight distribution
- Water surface election for hydrostatic force calculation
- Perturbation of hydrodynamic coefficient
- Difference in Sagging and Hogging conditions

The hull shape and weight distribution are defined by the geometry, structure and loading condition of the ship. Given the mature 3D modeling module in *Napa*, the quality in the hull shape and weight distribution is quite reliable. The water surface election makes it different in the computational time between strip method and panel method, because for the strip method, the real calculation is only for several sections, while for the panel method, the calculation shall be done for each of the panel close to the water surface, depending on the density of defined panels. The perturbation of hydrodynamic coefficient is a compromising way to take into consideration the wave election impact on disturbance potential. *Napa* tries to convert the high-order linear terms into linear terms to reduce the difficulty in calculation and increase the accuracy to some extent. The difference in sagging and hogging conditions is really important for structrual design. In a simulation work, it is essential for the loads study.

Since the focus of the work is on the early ship design, the nonlinearities considered by *Napa* is surficient. The problem can be solved in the frequency domain, and the accuracy is adequate to predict the ship motions and loads on hull girder. Comparing with panel method, the strip method is simpler and more stable in *Napa*. Thus, strip method is mainly studied in this thesis work. Given that he ship motion prediction is quite mature, the focus of the work is put on the hull girder loads, including vertical bending moment and shear force.

Besides the methods in hydrodynamic force calculation, the ship service condition is also important in the thesis work. Methods in describing the sea states and wave conditions are to study and introduced in the thesis. The ship response in vertical bending moment can then be calculated.

For the vertical bending moment and shear force, each ship class society has its own rule in the requirement. The results calculated by *Napa* shall be taken into compare with some rules. Among the ship class societies, the DNV-GL rule and IACS rule are picked to study, since they are more generally used and recogonized. The difference between the two rules and the computed results shall be studied and analyzed. A mutual justification is part of the scope in the thesis project.

1.4 Aim of the thesis

The target of this thesis project is to suggest a practical way to calculate the wave vertical bending moment and shear force during the early design stage. The validation of the method and the rule requirement shall be discussed. Based on this aim, the two research questions are focused to answer:

- How valid the DNV-GL rule and IACS rule are in requiring wave vertical bending moment and shear force along the ship?
- How feasible *Napa* is in checking the loads on ship hull girder during early design stage?

To achieve the goal, the worst case in the vertical bending moment that the ship could face shall be found out according to the simulation results in certain wave conditions. After that, the vertical bending moment and shear force along the ship shall be calculated in that worst case. The loads are then compared with the DNV-GL and IACS rules. The formulation in DNV-GL shall be studied. The differences between different rules shall be discussed and the validation shall be commented.

Besides, the thesis work is done for Department of Mechanical Engineering, Aalto University. Another aim of the thesis work is to provide a practical process for students in Naval Architecture to understand more in structural design. The right to use of *Napa* is available in Aalto University and many course projects are carried on with *Napa*. Students usually follow their study plan and try to experience the whole design process. Nowadays, according to the teaching progress, students have their ship models built and learn the stability and seakeeping calculation in *Napa*, also with the aid of *Matlab*. This thesis work aims to help the students learn the ship design progress in a more completed scale.

2 Methodology

2.1 Wave

Ocean surface waves are the reason that introduce periodic loads on any object in the sea, no matter it is a kayak, a ship or an offshore structure, even a rod floating on the sea surface. To design a ship, it is important to learn the loads. Thus, the source of them, waves, are crucial to be studied.

2.1.1 Wind-induced wave

When looking at the sea, irregular humps and hollows are always obviously moving from one direction to another. Not thinking about the interaction from islands or other objects, the waves are created by the wind. When there is light wind, the wave condition could look relatively regular. When the wind blows strong and perhaps with changeable directions, a terrible stormy sea state might appear, with very irregular waves on the surface. The waves usually transfer easily and calm water can rarely be observed. Even when a smooth sea surface is observed, it could still be a wave with the wavelength which is too long to be captured. Since the obstruction of wave propagation is unpredicable, it is reasonable to take into consideration only the waves induced by the wind during early design stage.

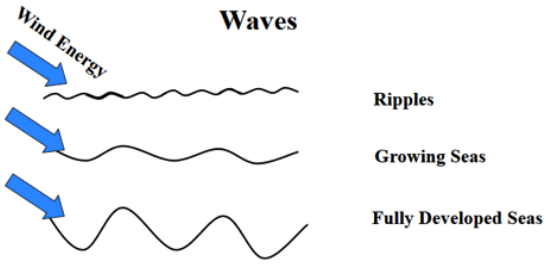

Figure 6: Wind-induced wave conditions.*[57]*

Figure 6 indicates the wave conditions induced by wind. The wave starts to appear because of the wind blow on a glassy surface. The frictional forces between wind and water transfers part of the energy from the wind into the water. Ripples arise in the first stage due to irregularities in the speed and direction of the wind. As soon as the ripples appear, the wind is then able to transfer the energy by providing pressure directly on the wave crests. The energy goes easier from the wind to the water and the wave keeps growing. Until the ripples have too much height referring to their length, they start to break into wave with longer wave length and lower height. More wind energy is able to be transferred until the forms a more rounded shape. This kind of wave is so-called *gravitational waves.[1]*

Thus, the wave loads can be defined as different forms of energy. For waves which are strong enough to cause influence on vessels, the motion of them is driven by the interaction between gravitational potential energy and kinetic energy, hereby the term *gravity waves*. When the wave has equal speed as the wind in the same

direction, no further energy transfer is possible. The wave length and wave height are constant over time as long as the wind speed remains constant. The sea state becomes stationary and is called a *fully developed sea state.[1]*

2.1.2 Regular wave

As a rule of thumb, the sea water surface always rises to the crest and falls to the trough around a mean water level. Meanwhile, the wave propagates from one direction to another. The wave with fixed vertical wave surface position ζ, wavelength λ and peak period T is regarded as regular wave. Figure 7 shows a snap shot of a regular wave propagating.

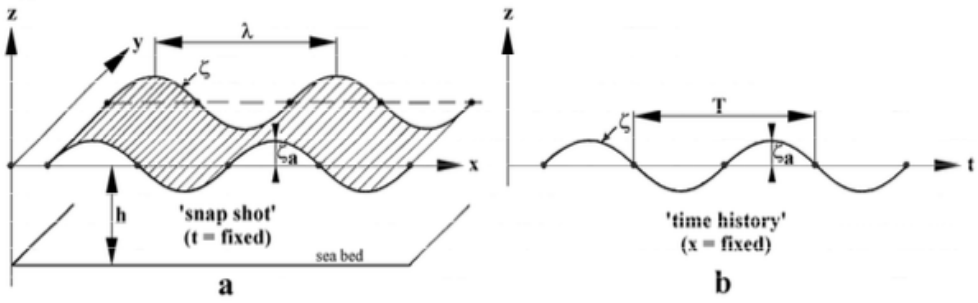

Figure 7: A snapshot of a regular wave.*[23]*

Hereby, *Stokes wave* shall be introduced. *Stokes wave* is a model raised by *Sir George Stokes*. It is a description of low-order nonlinear wave in intermediate and deep water. It was proved to exsit and dominate in most developed sea states. It is now widely used in the design of ships and offshore structures, in order to determine the wave kinematics, which is very important for the wave loads study*[61]*. There are some assumptions and restrictions upon *Stokes wave*:

- The water is assumed to be modeled as an ideal fluid.
- Gravity is the only external force working on the wave.
- The pressure on the wave surface is constant.
- The wave amplitude is finite. The upper limit of the wave steepness is set at $H/\lambda = 1/7$.

With these assumptions, and hence, limiting the wave expression to be linear, a solution to *Laplace equation* (Equ. 22) can be found and the wave surface is obtained according to:

$$\zeta(x,t) = \zeta_0 \cos(kx - \omega t + \varepsilon^{\zeta}) \tag{1}$$

where ζ is the vertical position of the wave surface relative to the calm water level, x is a space coordinate and t is time. A regular wave can thus be obtained in a space coordinate or a time domain as shown in Figure 8.

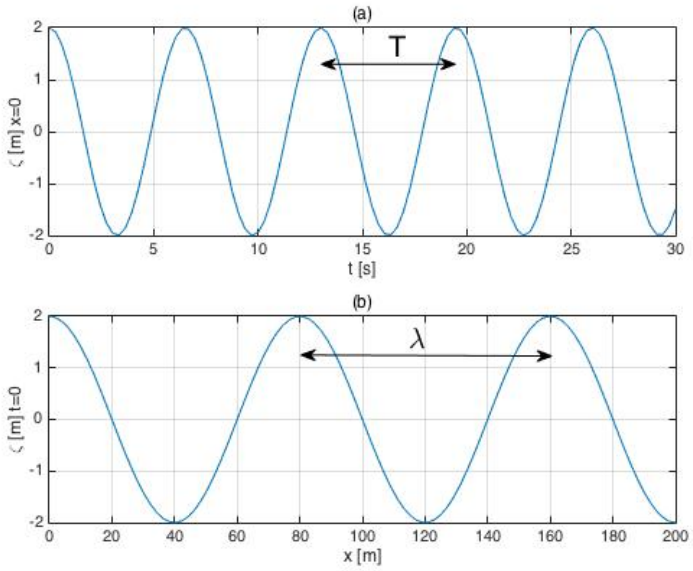

Figure 8: Regular wave plotted (a) for a certain point over a period of time ($0 < t < 30, x = 0$), and (b) in a certain moment over a distance ($0 < x < 200, t = 0$). $\zeta_0 = 2m$; $\varepsilon^\zeta = 0$; $T = 6.5s = 2\pi/\omega \Rightarrow \omega = 0.97s^{-1}$; $\lambda = 80m = 2\pi/k \Rightarrow k = 0.0785m^{-1}$.

In Figure 8, ζ_0 is the wave amplitude, the vertical distance between the 0-level and wave trough and wave crest. The wave height H is defined as the distance between the adjacent wave trough and wave height. For regular waves, $H = 2\zeta$. ε^ζ is the phase shift that determines the level at $t = 0$ and $x = 0$, with a range $-\pi \leq \varepsilon^\zeta \leq \pi$.*[1]*

Table 3: Coefficient relations for regular gravity waves in deep waters (Huss 1983)*[62]*.

	λ	T	c	k	ω
λ	λ	$\frac{gT^2}{2\pi}$	$\frac{2\pi c^2}{g}$	$\frac{2\pi}{k}$	$\frac{2\pi g}{\omega^2}$
T	$\sqrt{\frac{2\pi\lambda}{g}}$	T	$\frac{2\pi c}{g}$	$\frac{2\pi}{\sqrt{gk}}$	$\frac{2\pi}{\omega}$
c	$\sqrt{\frac{\lambda g}{2\pi}}$	$\frac{gT}{2\pi}$	c	$\sqrt{\frac{g}{k}}$	$\frac{g}{\omega}$
k	$\frac{2\pi}{\lambda}$	$\frac{4\pi^2}{gT^2}$	$\frac{g}{c^2}$	k	$\frac{\omega^2}{g}$
ω	$\sqrt{\frac{2\pi g}{\lambda}}$	$\frac{2\pi}{T}$	$\frac{g}{c}$	$\sqrt{gk}$	ω

Here, Table 3 from Huss*[62]* indicates the relations between all the coefficients of regular waves. Among those, c is the wave propagation speed, also know as phase velocity.

2.1.3 Irregular wave

Due to the instability of the wind, the fully developed waves are normally characterized by great *irregularity* and *randomness*. These two characters actually highly increase the difficulty in describing the sea state. A picture of how the fully developed sea surface looks like after hours of blow by the 5 m/s wind is shown in Figure 9. To deal with this, a method shall be taken from electromagnetism that the irregular wave is regarded as the superposition of regular waves. This method is feasible as long as the wave composition is assumed linear.

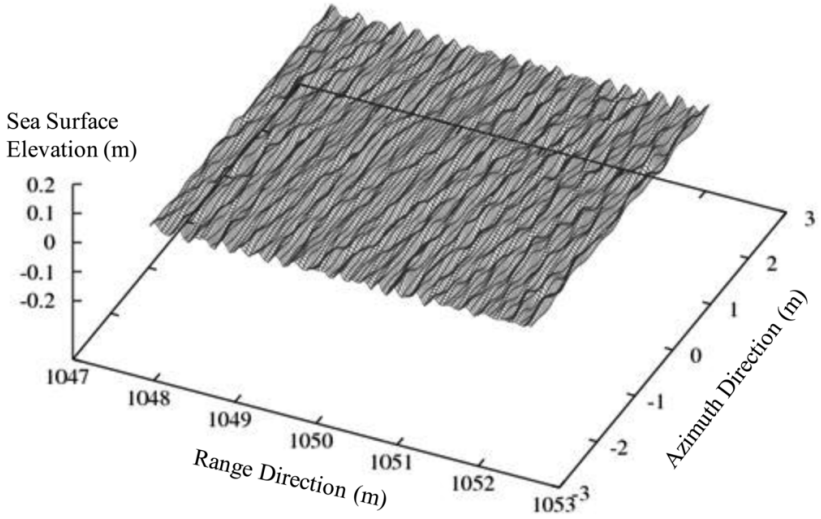

Figure 9: Example of numerical sea surface for irregular wind wave (wind speed 5 m/s).*[59]*

Figure 10 illustrates how an irregular wave is made up with by a sum of regular waves. The irregular wave (e) is composed by regular wave (a)-(d). In reality, the irregularity of waves is heavier, but there is always a way to simulate the irregular wave with the superposition of plenty of regular waves. To express the irregular wave as a formulated form:

$$\zeta = \zeta_1 + \zeta_2 + ... + \zeta_M \tag{2}$$

With the superposition principle, the irregular wave kinematics can also be determined by considering that of each regular wave separately. However, to capture the kinematics of irregular wave in time domain is not better than to do it in the frequency domain, because the hydromechanics of the ship is much easier to be calculated in the frequency domain. Thus, a method to transform the irregular wave from time domain to frequency domain is required.

2.1.4 Transform between different domains

As mentioned in the earlier chapter, comparing with frequency domain, time domain is usually time consuming and inconvenient for the seakeeping calculation. For *Napa*,

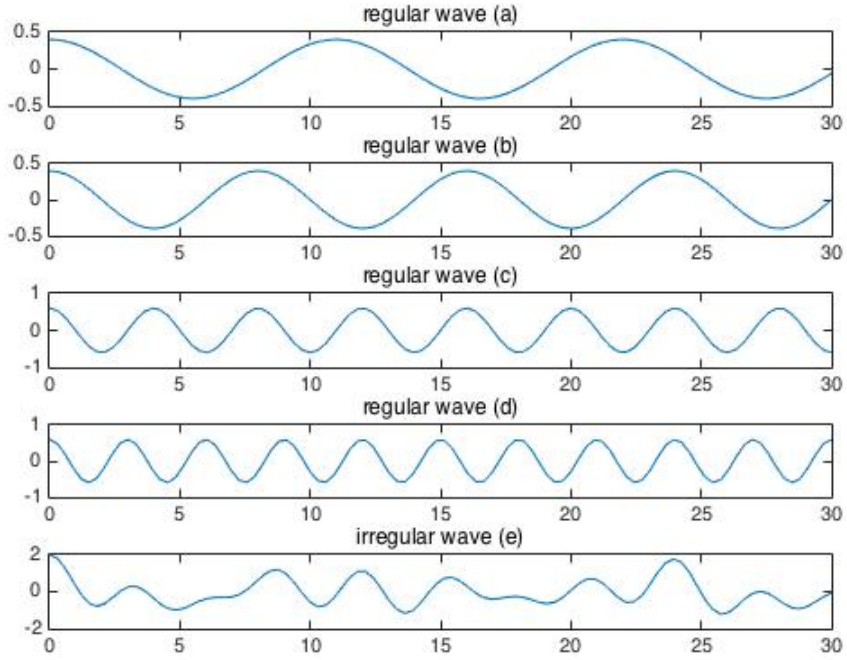

Figure 10: A sum of simple sine waves makes an irregular sea. The irregular wave (e) is composed by regular wave (a)-(d).

it is also the frequency domain that is applied for calculation. Thus, it is essential to convert the time-domain information into frequency domain. Hereby, an applicable method shall be introduced, which is so-called $Fourier\ transform$.

The $Fourier\ transform$ decomposes a function of time into the frequencies that make it up. The Fourier transform of a function of time itself is a complex-valued function of frequency. Its absolute value represents the amount of that frequency present in the original function, and its complex argument is the phase offset of the basic sinusoid in that frequency*[58]*. Figure 11 indicates how sea state can be tranformed from time domain to frequency domain and vice versa.

Besides the frequency domain and time domain, there is another domain, which is so-called probability domain. The relationship between the domains can be seen in Figure 12. The probability domain represents the times of appearance of waves within a period of time. It is more related to data collection and statistics. The probablity domain is like a bridge, which connects the information in reality with the computable data. With the help of probablity domain, the information of the sea states can be collected as statistic chart and converted for the frequency-domain calculation.

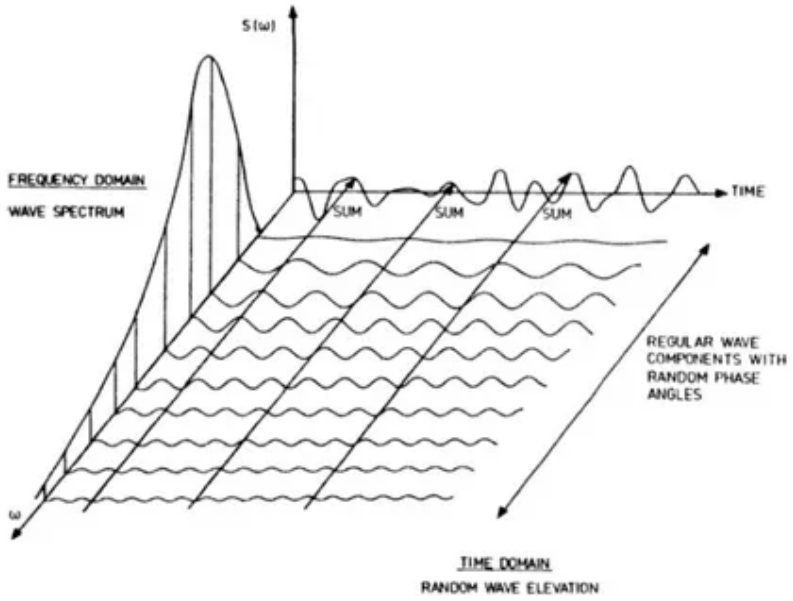

Figure 11: An illustration about how sea state can be tranformed between time domain and frequency domain by Fourier transform.*[60]*

2.1.5 Wave statistics

To capture the feature of irregular waves, the probability domain is applied to present the information of irregular waves. Figure 13 indicates the two important parameters of irregular waves, the wave height $H1$-$H4$ and corresponding zero crossing period $T1$-$T4$. The wave condition shall be taken in a period of time. Data can thus be collected. As a clear present, time intervals are set. Within each intervals, the *mean crossing period* T_z can be calculated according to Equ. 3. The mean value of 1/3 of largest wave height can also be defined as *significant wave height* $H_{1/3}$ and determined according to Equ. 4. The number of appearance referring to each zero crossing period and significant wave height can then be reported in a table.

$$T_z = \frac{\sum_{n=1}^{N} T_{z,N}}{N} \tag{3}$$

$$H_{1/3} = \frac{\sum_{n=N-N/3}^{N} H_n}{N/3} \tag{4}$$

Hogben et al.*[64]* divided the sea and ocean states all over the world into several areas geographically. Sea states can then be studied separately and provided for ship design. The separation is illustrated in Figure 14.

Among all those areas, the North Atlantic Sea is recognized to be the most severe sea state. Thus, for ship working in unlimited service area, the wave condition in North Atlantic Sea is usually taken for seakeeping calculation, which is Area 9. The wave statistics for the area is shown in Table 4. Table 4 illustrates the sea condition in Area 9 in eight directions. To make the problem easier, the all direction statsic chart is taken into use in this thesis project.

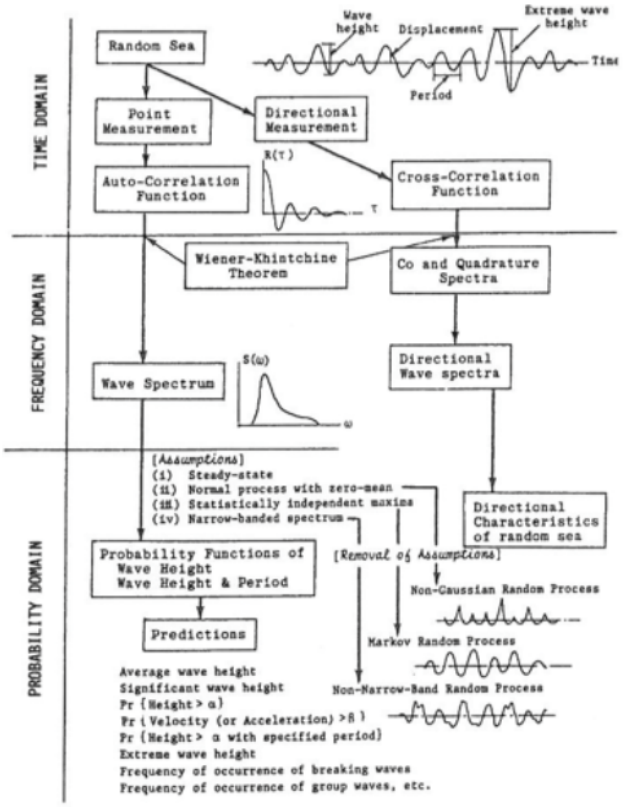

Figure 12: An illustration of the relationship in between time domain, frequency domain and probability domain.*[65]*

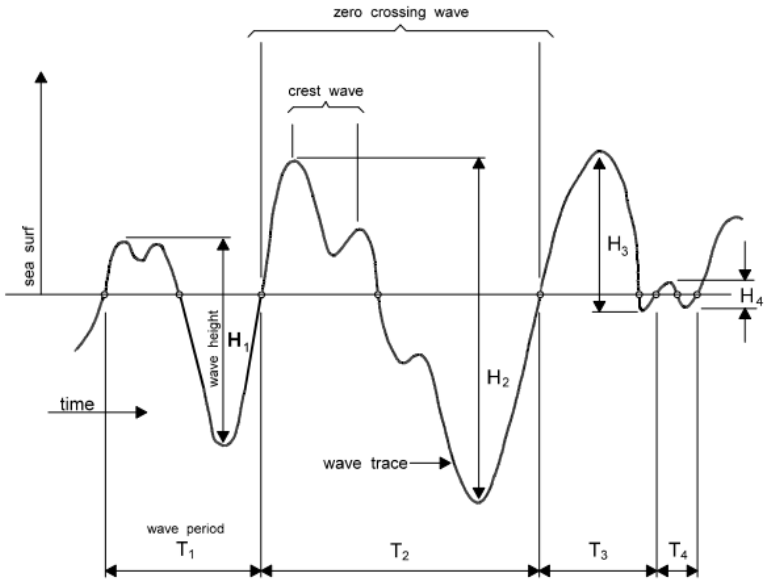

Figure 13: An indication of the parameters for and irregular wave.*[63]*

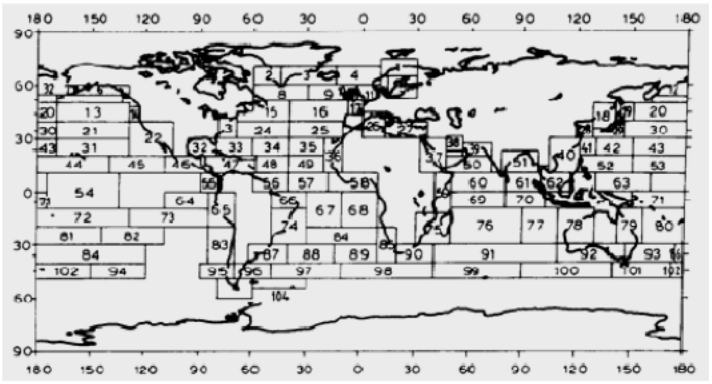

Figure 14: Geographical areas according to the wave statistics in Hogben et al (1986). *[64]*

Table 4: Wave statistics for Area 9 according to Hogben et al (1986).*[64]*

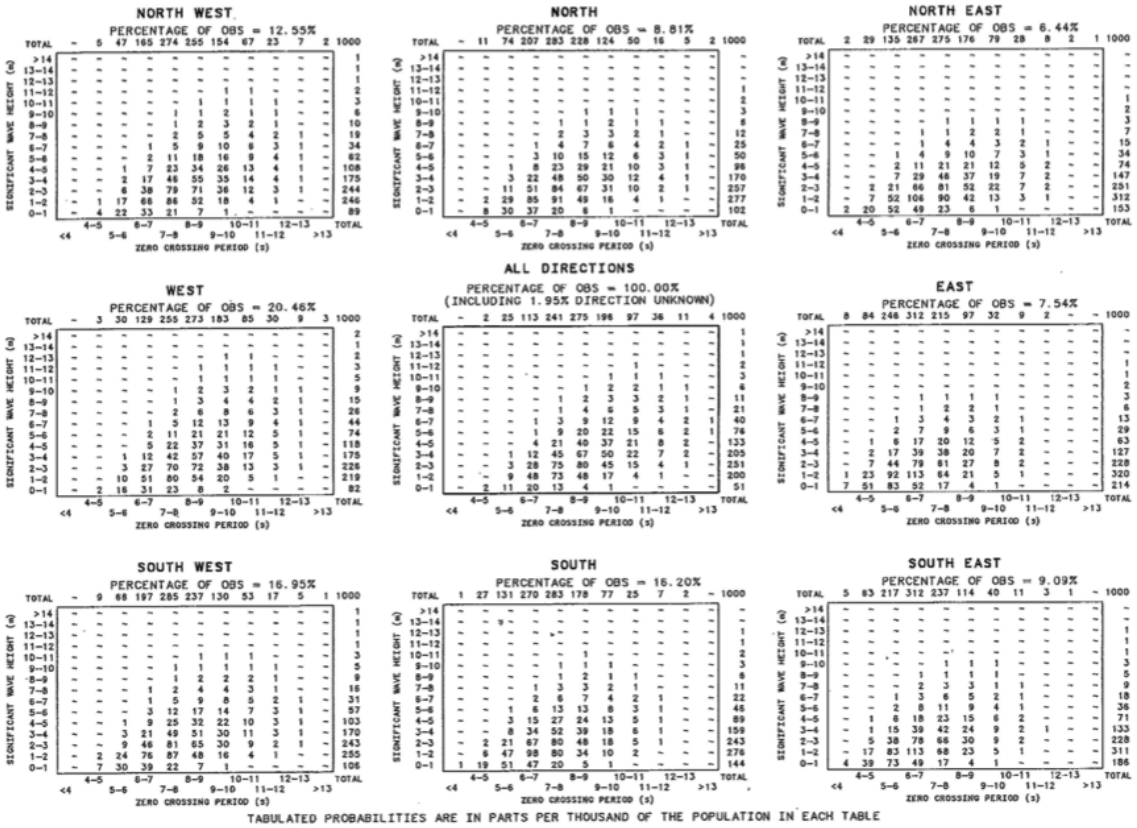

2.1.6 Wave spectrum

To apply the information in prabability domain, wave spectrum shall be employed, which convert the wave information to the frequency domain. Wave spectrums are used to represent how the energy is distributed on different frequencies in the sea state. A general representation of an irregular seastate is a *continuous energy spectrum* formulated as:

$$S_\zeta(\omega) = 0.5\zeta_0^2/\triangle\omega; \qquad \triangle\omega \to 0 \tag{5}$$

And hence:

$$\zeta_0 = \sqrt{2 \cdot S_\eta(\omega_m) \cdot \triangle\omega} \tag{6}$$

Michel K. Ochi*[65]* concluded four kinds of wave spectrums which are normally taken into use. The four kinds of spectrums differ in number of parameters. They are Pierson-Moskowitz Spectrum, Two-Parameter Spectrum, Six-Parameter Spectral family and JONSWAP Spectrum. The main difference between spectrums is the scope of application. In this project, the ISSC spectrum, introduced in the following paragraphs, is selected, since it is recogonized by the authorities.

Pierson-Moskowitz spectrum
In *Pierson-Moskowitz spectrum*, the mean wind speed at 19.5 meter height above sea level is considered to be the only input of the spectrum formula. The formula can be written as*[65]*:

$$S_\zeta(\omega) = \frac{0.0081g^2}{\omega^5} e^{-0.74(\frac{g/U_{19.5}}{\omega})^4} \tag{7}$$

Where $U_{19.5}$ is the mean wind speed at 19.5 meter height above sea level. This spectrum is rather simple and feasible, but it is only valid for fully developed sea state.*[65]*

Two-parameter spectrum
In order to represent fully as well as partially developed wind-generated seas, a two-parameter spectrum was developed by Bretschneider in 1959*[66]*. The formula can be written as:

$$S_\zeta(\omega) = \frac{0.3125\omega_m^4}{\omega^5} H_{1/3}^2 e^{-1.25(\frac{\omega_m}{\omega})^4} \tag{8}$$

Where $H_{1/3}$ is the significant wave height and ω_m is the wave modal frequency, defined as $\omega_m = 0.4\sqrt{g/H_{1/3}}$. This original formulation has not been widely used in practice, but the concept of wave spectrum defined by two parameters has significantly contributed in the development of several formulations. The International Ships & Offshore Structures Congress (ISSC) and the International Towing Tank Conference (ITTC) published their empirical two-parameter wave spectrum formulation*[1]*:

$$S_\zeta(\omega) = \frac{A}{\omega^5} e^{-B/\omega^4} \tag{9}$$

Where A and B are expressed in terms of different coefficients according to Table 5. Since the sea wave statistic chart offers the direct information in terms of significant wave height and mean zero period, the two-parameter spectrum is very handy.

Table 5: Coefficients for different variants of ISSC and ITTC wave spectrum. $H_{1/3}$ is the significant wave height and T_z is the zero crossing period.*[1]*

Spectrum	A	B
ISSC	$124H_{1/3}^2/T_z^4$	$494/T_z^4$
ITTC	$0.0081g^2$	$3.11/H_{1/3}^2$

Six-parameter spectral family

This formulation carries six parameters, but in reality significant wave height is the only input to the formulation. The advantage of using a family of spectra for design is that each family member yields response to a particular extent. The smallest response has a confidence coefficient of 0.95 comparing with the largest. Thus, by connecting the largest and smallest values, the upper and lower-bounded response can be established in each sea severity.*[65]*

$$S_\zeta(\omega) = 0.25 \sum_j \frac{[(4\lambda_j + 1)\omega_{mj}^4/4]^{\lambda_j}}{\Gamma(\lambda_j)} \frac{H_{sj}^2}{\omega^{4\lambda_j} + 1} e^{-[\frac{4\lambda_j+1}{4}][\frac{\omega_{mj}}{\omega}]^4} \tag{10}$$

where $j = 1$ and 2 and the parameters are picked according to Table 6.

Table 6: Parameters of six-parameter family spectra (From Ochi and Hubble 1976). *[65]*

	H_{s1}	H_{s2}	ω_{m1}	ω_{m2}	λ_1	λ_2
Most probable spectrum	$0.84\ H_s$	$0.54\ H_s$	$0.70\ e^{-0.046\ H_s}$	$1.15\ e^{-0.039\ H_s}$	3.00	$1.54\ e^{-0.062\ H_s}$
0.95 confidence spectra	$0.95\ H_s$	$0.31\ H_s$	$0.70\ e^{-0.046\ H_s}$	$1.50\ e^{-0.046\ H_s}$	1.35	$2.48\ e^{-0.102\ H_s}$
	$0.65\ H_s$	$0.76\ H_s$	$0.61\ e^{-0.039\ H_s}$	$0.94\ e^{-0.036\ H_s}$	4.95	$2.48\ e^{-0.102\ H_s}$
	$0.84\ H_s$	$0.54\ H_s$	$0.93\ e^{-0.056\ H_s}$	$1.50\ e^{-0.046\ H_s}$	3.00	$2.77\ e^{-0.112\ H_s}$
	$0.84\ H_s$	$0.54\ H_s$	$0.41\ e^{-0.016\ H_s}$	$0.88\ e^{-0.026\ H_s}$	2.55	$1.82\ e^{-0.089\ H_s}$
	$0.90\ H_s$	$0.44\ H_s$	$0.81\ e^{-0.052\ H_s}$	$1.60\ e^{-0.033\ H_s}$	1.80	$2.95\ e^{-0.105\ H_s}$
	$0.77\ H_s$	$0.64\ H_s$	$0.54\ e^{-0.039\ H_s}$	0.61	4.50	$1.95\ e^{-0.082\ H_s}$
	$0.73\ H_s$	$0.68\ H_s$	$0.70\ e^{-0.046\ H_s}$	$0.99\ e^{-0.039\ H_s}$	6.40	$1.78\ e^{-0.069\ H_s}$
	$0.92\ H_s$	$0.39\ H_s$	$0.70\ e^{-0.046\ H_s}$	$1.37\ e^{-0.039\ H_s}$	0.70	$1.78\ e^{-0.069\ H_s}$
	$0.84\ H_s$	$0.54\ H_s$	$0.74\ e^{-0.052\ H_s}$	$1.30\ e^{-0.039\ H_s}$	2.65	$3.90\ e^{-0.085\ H_s}$
	$0.84\ H_s$	$0.54\ H_s$	$0.62\ e^{-0.039\ H_s}$	$1.03\ e^{-0.030\ H_s}$	2.60	$0.53\ e^{-0.069\ H_s}$

JOWSWAP spectrum

JOWSWAP spectrum formulation is based on an extensive wave measurement program known as the Joint North Sea Wave Project. It represents wind-generated

seas with a fetch limitation, and thereby wind speed and fetch length are inputs to this formulation. The JONSWAP spectrum can be obtained for a specified sea severity and fetch length.*[65]*

$$S_\zeta(f) = \alpha \frac{g^2}{(2\pi)^4} \frac{1}{f^5} e^{-1.25(f_m/f)^4} \gamma^{e^{-(f-f_m)^2/2(\sigma f_m)^2}} \tag{11}$$

where

γ	=	peak-shape parameter, 3.30 as an average
α	=	$0.076(\bar{x})^{-0.33}$
σ	=	0.07 for $f \leq f_m$, and 0.09 for $f > f_m$
f_m	=	$3.5(g/\bar{U})(\bar{x})^{-0.33}$
$\bar{x}$	=	dimensionless fetch $= gx/\bar{U}^2$, x = fetch length, and $\bar{U}$ = mean wind speed.

2.2 Ship behavior in regular waves

When a ship is traveling through waves at sea, there is always interaction between the ship hull and the waves. The interaction leads to oscillating hydromechanical pressure on the hull surface and oscillation in ship motions. The ship response shall be estimated in accordance with the wave information and ship mechanical properties. When designing a ship, it is wise to foresee the loads on the ship and its performance in different situations and define the seaworthiness of the ship.

In this section, the calculation method for ship behavior is presented. Some of the application is done with Napa, which has its own code in the behinde. The detailed codes are unavailable but the principles are introduced.

To estimate the ship behavior in regualr waves, the coordinate fixed on the ship's center of gravity (CoG) shall be clarified first, which is called $body-bound$ coordinate system $G(x_b, y_b, z_b)$. The ship motions are defined in the six degree of freedom (DoF) around CoG as shown in Figure 15.

Three of them are in the direction of the $x-$, $y-$ and $z-$axes:

- *Surge* in the longitudinal $x-$direction, positive forwards.
- *Sway* in the lateral $y-$direction, positive to port side.
- *Heave* in the vertical $z-$direction, positive upwards.

The other three are the rotations about the axes:

- *Roll* about the $x-$axis, positive right turning.
- *Pitch* about the $y-$axis, positive right turning.

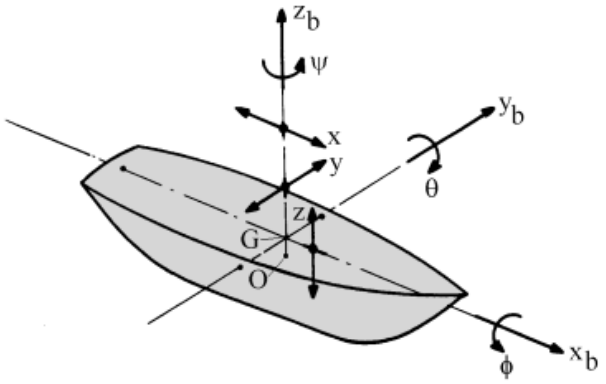

Figure 15: Definition of ship motions in six degrees of freedom.*[1]*

– Yaw about the $z-$axis, positive right turning.

Besides the $body-bound$ coordinate system, there is another coordinate system, which is the $earth-bound$ coordinate system $S(x_0, y_0, z_0)$. The plane (x_0, y_0) lies on the still water surface, with the positive x_0-axis in the direction of the wave propagation. It can be translated to the $body-bound$ coordinate system by rotating and angle of μ. An indication about the relation between the $body-bound$ coordinate system and the $earth-bound$ coordinate system is shown in Figure 16.

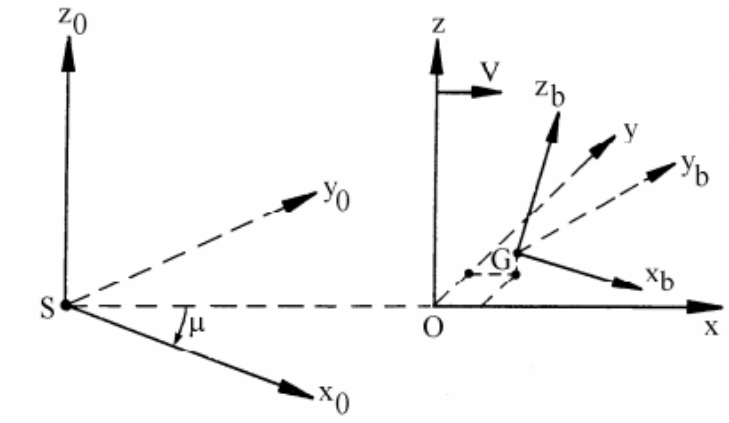

Figure 16: Relation between the $body-bound$ coordinate system and the $earth-bound$ coordinate system. *[23]*

The wave motion mentioned in Equ. 1 is in the $earth-bound$ coordinate system. According to Newton's second law, in the $earth-bound$ axes system, the equations of motion of an oscillating ship in waves are written as:

$$\sum_{j=1}^{6} (M_{ij} + A_{ij}) \cdot \ddot{\eta}_i + B_{ij} \cdot \dot{\eta}_i + C_{ij} \cdot \eta_i = F_i \qquad (i = 1, ...6) \tag{12}$$

η_i with indices $i = 1, 3, 5$ are the displacement of CoG (surge, sway and heave), while x_i with indices $i = 2, 4, 6$ are the rotations against the axes (roll, pitch and yaw). F_i is sum of the loads in each DoF, which is composed by the radiation force F_i^{sw} and the hydrodynamic force F_i^{wm}. M_{ij}, A_{ij}, B_{ij} and C_{ij} are the *mass*, *added mass*, *damping* and *spring* respectively. The indices ij represents the coupling terms between motion i and motion j.

The solution of EoM shall be derived in frequency domain by a proper ansatz, either on amplitude-phase form or on complex form. Amplitude-phase form:

$$\eta_i = \eta_{i0} \cdot cos(\omega_e t + \epsilon_i) \tag{13}$$

Complex form:

$$\eta_i = \hat{\eta}_i e^{i\omega_e t} \tag{14}$$

Where η_{i0} is the amplitude of motion in the degree of freedom i. ω_e is the frequency of encounter. In deep water, it can be expressed as:

$$\omega_e = \omega - \frac{\omega^2}{g} V cos(\mu) \tag{15}$$

To solve the EoM, the problem is turned into obtaining the coefficients and hydromechanical force and moment. A practical way is to separate the hydrodynamic model into two sub-models. Figure 17 indicates how the ship motion problem can be solved by dividing it into two sub-models. In Figure 17, model i) is the ship free oscillation in calm water surface. It relates to the hydromethcnical forces and moments related to ship motions. In model ii), the ship is fixed, and the wave motion is applying loads on the ship. As illustrated in Figure 4, the composition of the hydrodynamic force can be described as the sum of radiation force, the Foude-krylov force and the diffraction force. In model i), the raditation force can be calculated, which relates to the ship mechanical property. In model ii), the Froude-krylove force and the diffraction force can be obtained, which is related to the wave loads introduced in the last section. With both models into consideration, the equation of motion can be derived, and model ii), the ship oscillation in waves can be estimated. Figure 17 shows model of ship rolling in beam seas, but actually, the principle works for all the motions in six DoF. The vertical bending moment and shear force can be derived with the same principle.

2.3 Strip method

The coefficients and the radiation force in Equ. 12 are related the ship mechanical properties. They are the target to be generated in model i), which can either be obtained by experiment or by simulation. The experiment approach, in most cases, gives fairly good picture, but it is rather time-consuming and expensive to carry out. Thus, the analytical or numerical approach is favoured in ealy design stage.

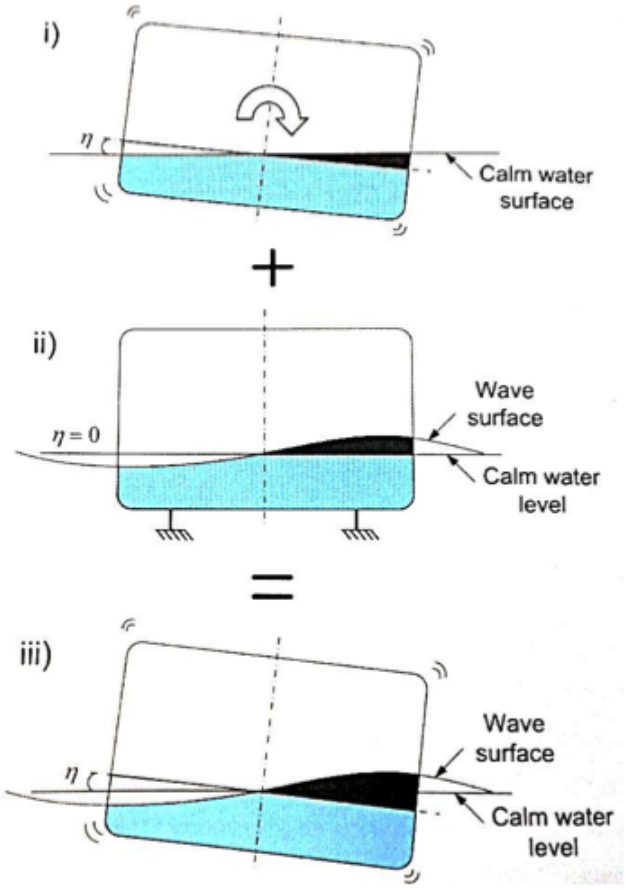

Figure 17: The interaction between wave load and ship motions.*[1]*

As mentioned, there are two ways in modeling the ship to obtain the ship mechancial properties, *strip method* and *panel method*. Since *Napa* is employed for the thesis project, the *strip method* is taken into use, which is most convenient, time-saving and stable in *Napa* calculation. The fundamental principle in *strip method* is to simplify the 3D hydromechanical model to 2D strips. In the application of *strip method*, the ship is required to have a slender body. Based on the assumption of slenderness, the wetted hull is replaced by cylinders in accordance with several strip sections along the longitudinal direction. The hydrodynamic force per unit length of these segments may then be calculated by assuming the cylinder infinitely long. Including the slenderness, there are some limitations in applying the strip method:

- Slender hulls, large ship length in relation to the breadth.
- High frequency, resulting in higher transverse flow speeds than longitudinal.
- Low speed, resulting in higher transverse flow speeds than longitudinal. Usually, the Froude number $Fn < 0.4$.

– Large wave length relative to the wave height, which has been mentioned in the linear wave theory.

– Small motions, to enable the approximation of the angular rotation.

2.3.1 Geometry

In Napa, 21 sections (20 segments) are defaulted and limited in describing a ship. The cross sections are assumed to be constant in each cylinder that they represent. The hull formed by strip method is shown in Figure 18. The strip-method hull is apparently not that exact comparing with the original hull, but in calculating the coefficients of equation of motion, this hull description makes the calculation easier and faster.

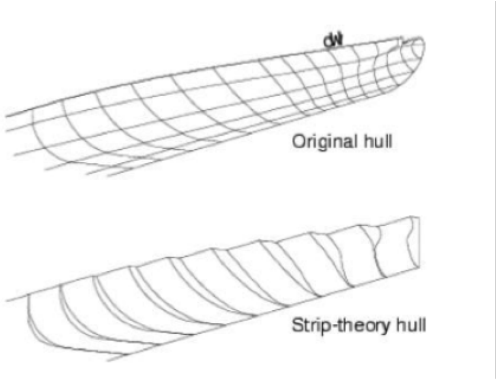

Figure 18: An illustration of the strip method, indicating how the 3D hydrodynamic problem can be converted to 2D problem.*[56]*

2.3.2 Lewis form

With several intervals in the longitudinal direction of the ship defined, a quick way in mapping the strips is employed. A popular way to map the strips is to regard the strips as a conformal mapping of a semi-cirle shape strip. A clear description regarding the comformal mapping is introduced by Journée and Adegeest*[23]*. An indication of the comformal mapping is shown in Figure 19. A general transformation formula is defined as*[23]*:

$$z = M_s \cdot \sum_{n=1}^{N} [a_{2n-1} \cdot \zeta^{-(2n-1)}] \tag{16}$$

Where z is the plane of ship's cross section indicated in Figure 19 (b).

$$z = x + iy \tag{17}$$

ζ is the semi-circle plane as shown in Figure 19 (a). The unit circle can be expressed as:

$$\zeta = ie^{\alpha} \cdot e^{-i\theta} \tag{18}$$

M_s is the scale factor. a_{2n-1} is the conformal mapping coefficients $(n = 1, ...N)$, and $a_{-1} = 1$, N is the maximum parameter index number.

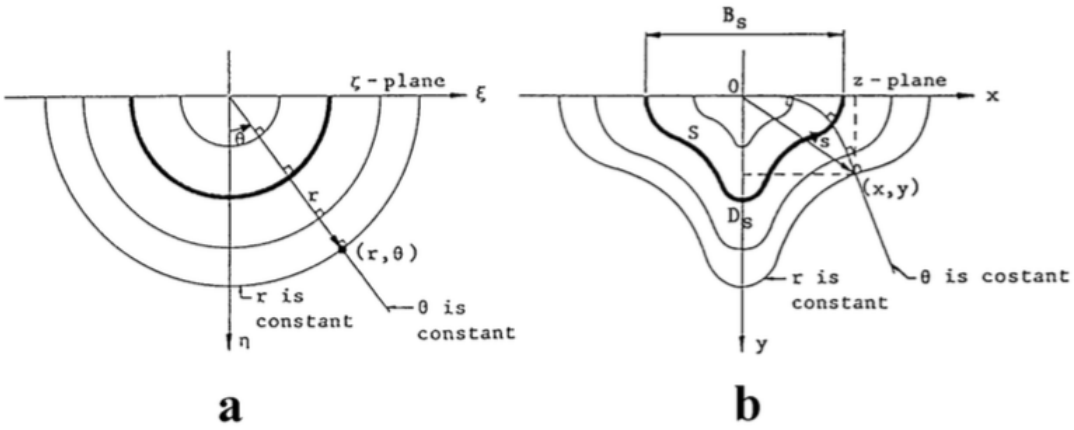

Figure 19: Comformal mapping between two planes.*[23]*

According to the User Manual of Napa*[56]*, a method called *Lewis transformation* is applied in mapping the strips. The two-parameter Lewis transformation of a cross section is defined by putting $N = 2$ into Equ. 16 and expressed as*[23]*:

$$z = M \cdot (a_{-1} \cdot \zeta + a_1 \cdot \zeta^{-1} + a_3 \cdot \zeta^{-3}) \tag{19}$$

And the integration of the Lewis form delivers the sectional area coefficient σ_s*[23]*:

$$\sigma_s = \frac{A_s}{B_s \cdot D_s} = \frac{\pi}{4} \cdot \frac{1 - a_1^2 - 3 \cdot a_3^2}{(1 + a_3)^2 - a_1^2} \tag{20}$$

Where A_s is the area of the cross section. B_s is the sectional breath on the water line. D_s is the sectional draught. a_1 and a_3 are so-called Lewis coefficients. Then the ship hull can be mapped according to B/D, σ_s and M. Some typical and realistic Lewis forms are presented in Figure 20.

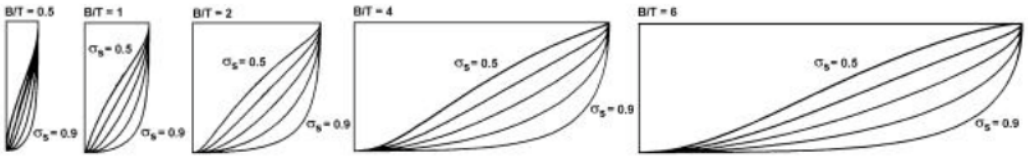

Figure 20: Typical Lewis forms.*[23]*

The use of Lewis-form ease the calculation for added mass and damping coefficients, but there are also some limitations in the application:

- The ship sections need to have a horizontal tangent at the baseline and a vertical tangent at the waterline to map a semicircle, while the actual sections not always fulfill this requirement, especially at the bow and stern sides of the ship. When meeting this situation, slight changes in the ship hull would be applied on. Fortunately, the changes bring little impact in the motions of normal ships.*[56]*
- The modeled ship hull is not exactly the same as the real hull form; especially in the bulbous bow the forms are approximated. *Napa* deals with this by varying the sectional area coefficient automatically in the program to avoid knuckles and loops. The way in modeling the ship hull is still valid for Lewis-form. Comparing with the overall performance of the method in normal ships, the main dimensions, displacement and loading condition play a much larger part than small variations in sectional shape.*[56]*
- When calculating the ship mechanic property, the exciting force is calculated with respect to unit ship motion and the ship motion is assumed not to be disturbed by the incoming waves. This assumption is reasonable but not right in assessing relative motions between ship and water surface.*[56]*

2.3.3 Solving the coefficients of EoM

Before deriving the coefficients of EoM for the whole ship, the coefficients for each strip shall be derived first by assuming infinitely long cylinders. The coefficients in Equ. 12 are derived by assuming the ship to have a unit motion in each degree of freedom. The hydrostatic coefficients C_{jk} are derived by quasi-statically translating the hull. The hydrodynamic coefficients, added water mass A_{jk} and damping B_{jk} are derived by oscillating the hull in the respective DoF according to Equ. 21.

$$\eta_i = \eta_{i0} \cdot cos(\omega t) \tag{21}$$

The impact from ship to the wave appears in terms of energy transportation, and the flow field is presented as the velocity potential ϕ. The velocity potential shall be calculated by using *Laplace equation*:

$$\nabla^2 \phi = 0 \tag{22}$$

As soon as the velocity potential is obtained, the hydrodynamic pressure p can be determined according to the *Bernouilli equation* by omitting the term $0.5(\nabla\phi)^2$ and the term $\rho g z$ which is included in C_{jk}, since the water is modeled as an ideal fluid:

$$p = -\rho \frac{\partial \phi}{\partial t} \tag{23}$$

The hydrodynamic force and moment for each strip can thus be calculated by integrating the pressure at the strip boundary:

$$f = \int_S p(r_y n_z - r_z n_y) dS \tag{24}$$

Where S is the strip boundary, (r_y, r_z) is a vector pointing from the origin in the used coordinate system to a point of the hull surface and (n_y, n_z) is the hull surface normal in that point. According to *Newton Second Law*:

$$f_k = -a_{jk}\ddot{\eta}_k - b_{jk}\dot{\eta}_k \tag{25}$$

Where the two-dimensional added mass a_{jk} and damping b_{jk} for the strip are identified as the coefficients related to the *acceleration* and *velocity terms* respectively. The three-dimensional coefficients can then be obtained by integrating the two-dimensional coefficients over the ship length. The force and moment can be expressed along the ship length as indicated in Equ. 26 and Equ. 27.

$$Q_v = e^{-i\omega t} \int_{x_0}^{x_f} (\eta_3 - x\eta_5)[f_3 - \omega^2 m(x)]dx \tag{26}$$

$$M_v = -\int_0^{x_f - x_0} Q_v dx \tag{27}$$

2.3.4 Response Amplitude Operators (RAO's)

To present the ship properties in the frequency domain, there is a rather practical thinking, that the ship shall be regarded as an operator. The regular waves are regarded as input in the model, and the ship behavior is obtained as the output after the operator. An indication is illustrated in Figure 21. Thus, the ship mechanical properties are called *Response Amplitude Operators* $(RAO's)$ in terms of $transfer\ function$ and $phasefunction$. The $transfer\ function\ Y(\omega)$ is the response amplitude η_0 normalized with the wave amplitude ζ_0 as a function of the wave frequency ω. The $phasefunction$ indicates the phase angle as a function of the wave frequency ω.*[1]*

$$Y(\omega) = \eta_0/\zeta_0 \tag{28}$$

2.4 Ship response

As illustrated in Figure 21, the amplitude of ship response can be generated in terms as $response\ function$ as soon as the wave loads information is given in terms of the *wave spectrum* and the ship mechanical property is simulated in terms of $transfer\ function$. With Equ. 6 and Equ. 28, it can be derived that:

$$S_\eta(\omega) = Y(\omega)^2 \cdot S_\zeta(\omega) \tag{29}$$

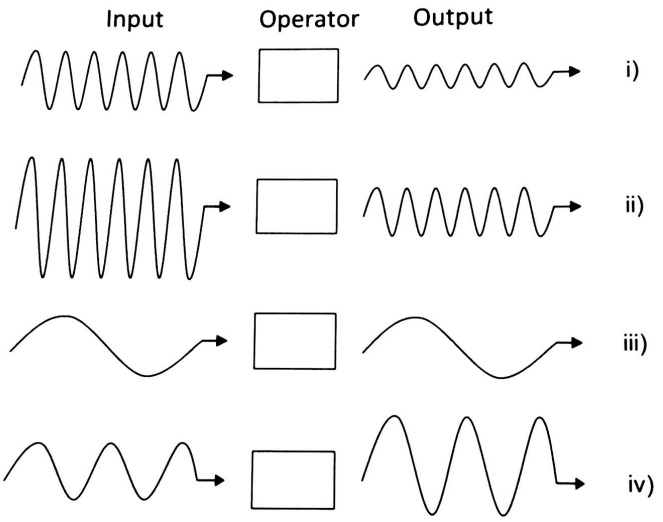

Figure 21: An indication of *Response Amplitude Operators.[1]*

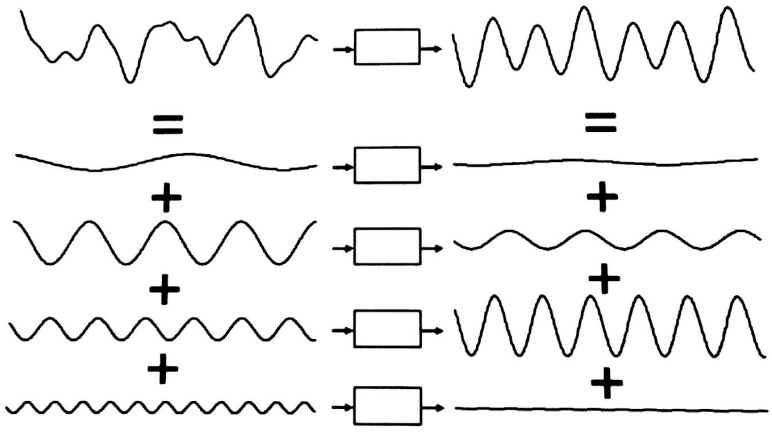

Figure 22: An illustration of how the ship response in irregular wave can be regarded as a sum of the response from several regular waves.*[1]*

Since the waves are regarded linear, and with Equ. 2, the ship response in irregular waves can also be regraded as the sum of the response from several regular waves*[1]*:

$$\eta(\zeta_1 + \zeta_2 + ... + \zeta_M) = \eta(\zeta_1) + \eta(\zeta_2) + ... + \eta(\zeta_M) \tag{30}$$

An indication is illustrated in Figure 22. In Figure 22, the left side indicates the composition of an irregular wave referring to Equ. 2. The box in the middle is the charactor of a ship, which is an operatoer. The right side indicates how the response against the irregular wave is composed by the sum of the responses of the regular waves, which compose the irregular wave. Thus, the amplitude of response in irregular waves shall be calculated as the standard deviation σ_η*[1]*:

$$\sigma_\eta^2 = \int_0^\infty S_\eta(\omega) d\omega \tag{31}$$

2.5 Rule requirement

Almost all the ship class societies have thier own rules in the requirement of loads on hull girder in terms of the vertical bending moment and shear force along the ship. $DNV-GL$ rule and $IACS$ rule are the authorities among all, which are taken for comparion with the calculated results. According to $DNV-GL$, *Part* 3, *Chapter* 4 *[67]*, the loads for strength assessment indlude Static and Dynamic load cases, where the static and dynamic loads are dependent on the loading condition being considered. The static load is estimated as the load in the still water while the dynamic load is composed by still water load and wave load. The static and dynamic loads are ruled in three aspects:

- Hull girder loads, including the vertical bending moment and shear force on hull girder.
- External loads, meaning the pressure on the hull.
- Internal loads, concerning the loads from inside of the ship.

In this thesis project, focus is put on the hull girder loads only. So, some descriptions in the loads on hull girder are to be introduced here. Before starting the description, the defination of sagging and hogging shall be clarified first. Hogging and sagging describe the shape of a beam or similar long object when loading is applied. Hogging describes a beam which curves upwards in the middle, and sagging describes a beam which curves downwards*[68]*. In Figure 23, diagram (1) represents the condition of hull sagging and diagram (2) illustrates the hull hogging condition under loads.

With the impact of sagging and hogging, the vertical bending moment and shear force cause the curve of the ship hull. Hereby, the defination for the positive and negative vertical bending moment M_v and shear force Q_v is illustrated in Figure 24. The vertical bending moments M_{sw} and M_{wv} are positive when they induce tensile stresses in the strength deck (hogging bending moment) and negative when they induce tensile stresses in the bottom (sagging bending moment). The vertical shear forces Q_{sw}, Q_{wv} are positive in the case of downward resulting forces acting aft of the transverse section and upward resulting forces acting forward of the transverse section under consideration*[67]*. The loads are then to be decribed in still water loads and wave loads separately, and the dynamic loads are the sum of them.

To make a clarification, the ship length in the rule is defined as indicated in $S2$ that the length of L is the distance, in metres, on the summer load waterline from the fore side of the stem to the after side of the rudder post, or the centre of the rudder stock if there is no rudder post. L is not to be less than 96%, and need not be greater than 97%, of the extreme length on the summer load waterline. In ships with unusual stern and bow arrangement the length L will be specially considered*[69]*.

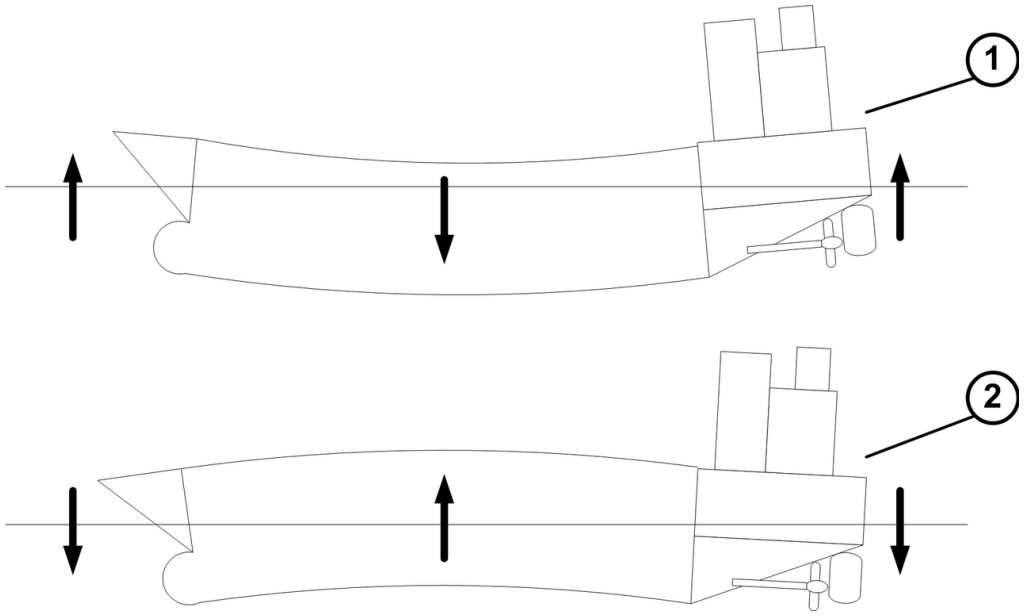

Figure 23: Diagram of ship hull (1) Sagging and (2) Hogging under loads.*[68]*

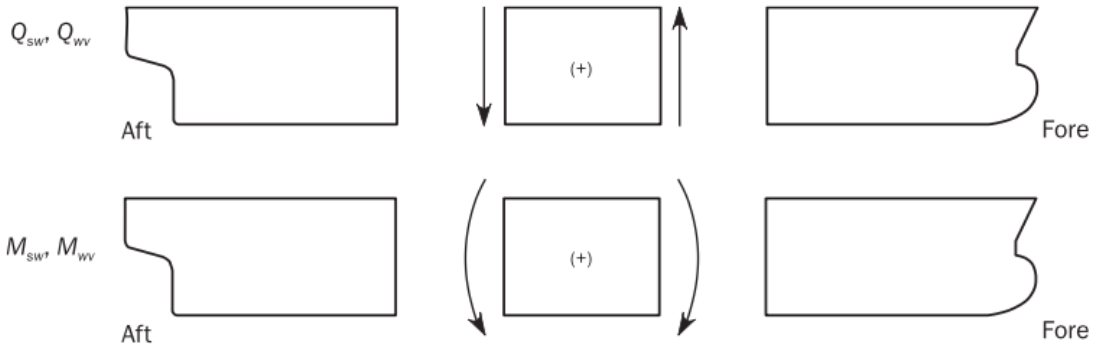

Figure 24: An indication of the positive and negative defination for vertical bending moment and shear force.*[67]*

2.5.1 Vertical still water bending moment

According to DNV-GL*[67]*, the still water vertical bending moment in seagoing condition is ruled, in kNm, at a preliminary design stage, for hogging and sagging respectively:

Hogging condition:

$$M_{SW-h-min} = f_{SW}(171C_W L^2 B(C_B + 0.7)10^{-3} - M_{WV-h-mid}) \tag{32}$$

Sagging condition:

$$M_{SW-s-min} = -0.85 f_{SW}(171C_W L^2 B(C_B + 0.7)10^{-3} - M_{WV-s-mid}) \tag{33}$$

where:

$M_{WV-h-min}$ and $M_{WV-s-min}$ are the maximum allowed vertical wave bending moment for strength assessment amidships in hogging and sagging condition, respectively. f_{SW} is the distribution factor along the ship length, see Figure 25*[67]*.

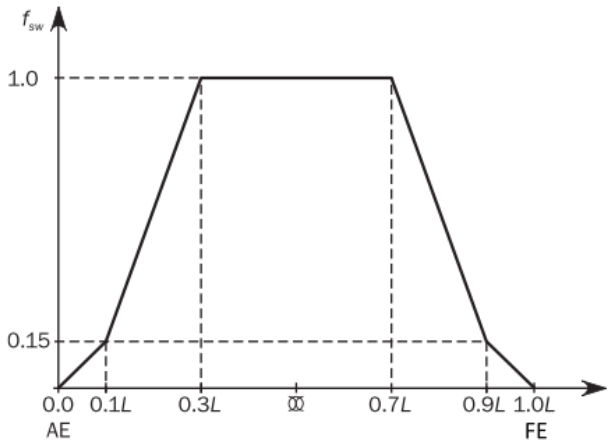

Figure 25: The distribution factor f_{SW} defined by DNV-GL.*[67]*

DNV-GL gives quite clear indication in the still water bending moment, while in IACS rule*[70]*, there is no clear indication, but still it is required to be checked as a case dependent issue.

2.5.2 Vertical wave bending moment

DNV-GL rule

According to DNV-GL*[67]*, The vertical wave bending moments at any longitudinal position is ruled in kNm as:

Hogging condition:

$$M_{WV-h} = 0.19 f_{nl-vh} f_m f_p C_W L^2 B C_B \tag{34}$$

Sagging condition:

$$M_{WV-s} = -0.19 f_{nl-vs} f_m f_p C_W L^2 B C_B \tag{35}$$

where:

f_{nl-vh} and f_{nl-vs} are coefficients considering nonlinear effects. They are taken as $f_{nl-vh} = 1.0$ and $f_{nl-vs} = 0.58(C_B + 0.7)/C_B$ respectively for strength assessment. f_p is the strenght assessment coefficient. $f_p = 1.0$ for ships operating in unlimited service area. C_W is the wave coefficient. For $L < 90$, $C_W = 0.0856L$. For $90 \leq L \leq 300$, $C_W = 10.75 - [(300 - L)/100]^{1.5}$. f_m is the distribution factor for vertical wave bending moment along the ship's length, see Figure 26*[67]*.

IACS rule

According to IACS rule, the wave bending moments, M_W, at each section along the ship length are given by the following formulae*[70]*:

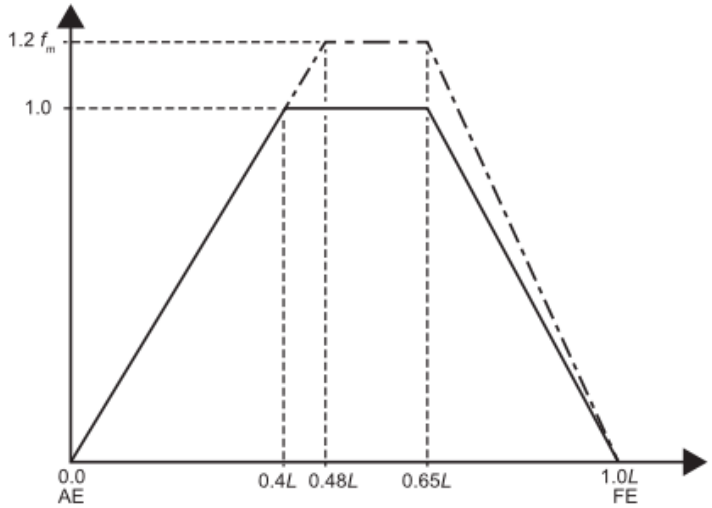

Figure 26: The distribution factor f_m defined by DNV-GL (solid line).*[67]*

For positive moment(Hogging):

$$M_W(+) = 0.19MCL^2BC_B \tag{36}$$

For negative moment(Sagging):

$$M_W(-) = -0.11MCL^2B(C_B + 0.7) \tag{37}$$

where:

M is the distribution factor, see Figure 27. C is the wave coefficient, in meters, related to the ship length L. For $90 \leq L \leq 300$, $C = 10.75 - [(300 - L)/100]^{1.5}$, but for $L < 90$, the value of C is not mentioned in $S11$, here C is taken the same as C_W from DNV-GL rule, $C = 0.0856L$ for $L < 90$.

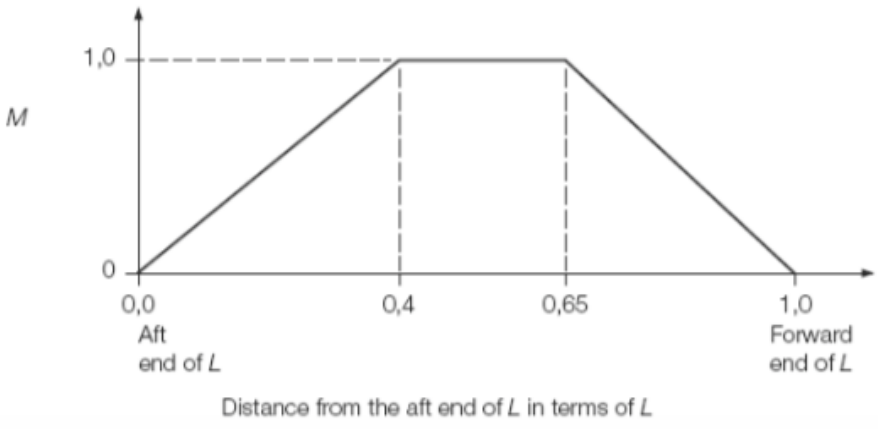

Figure 27: The distribution factor M defined by IACS.*[70]*

Comparing the requirement from DNV-GL in Equ. 34 and Equ. 35 with that from IACS in Equ. 36 and Equ. 37, it can be seen they are the same if f_{nl-h} in Equ. 35 is substituted in the term with C_B. Both of the equations take into consideration the nonlinearities in term of a factor. Actually, according to the report of Ship Structure Committee(SSC)*[71]*, in origin, $IACS$ took the requirement from the mean value from the rules of its 11 members. Those members have their own requirement based on different likelihood levels ranging from 10^{-4} to 10^{-8}. The mean estimated values gave a suggestion of mean likelihood of $10^{-5.4}$ for hogging and of $10^{-6.9}$ for sagging. In DNV rule, the probability level of the strength assessment is at 10^{-8}, which is the highest among all. Now $IACS$ also took this level since based on the quasi-statical analysis due to the appearance of large ships. The former estimation of waves height was set as $L/20$, which is too conservative for ship with large length. Thus, nowadays, C_W is adjusted to keep the likelihood a higher level*[71]*.

2.5.3 Vertical still water shear force

According to DNV-GL*[67]*, the still water shear force in seagoing condition is ruled at a preliminary design stage, in kN, for hogging and sagging respectively:

Positive condition:

$$Q_{SW-pos-min} = \frac{5 f_{qs} M_{SW-min}}{L} \tag{38}$$

Negative condition:

$$Q_{SW-neg-min} = \frac{-5 f_{qs} M_{SW-min}}{L} \tag{39}$$

where:

M_{SW-min} is the absolute maximum of $M_{SW-h-min}$ and $M_{SW-s-min}$ with $f_{SW} = 1.0$. f_{qs} is the distribution factor along the ship length, taken as:

$f_{qs} = 0.0$ for $x \leq 0$

$f_{qs} = 1.0$ for $0.15 \leq x \leq 0.3$

$f_{qs} = 0.8$ for $0.4 \leq x \leq 0.6$

$f_{qs} = 1.0$ for $0.7 \leq x \leq 0.85$

$f_{qs} = 0.0$ for $x \geq L$

Intermediate values of f_{qs} shall be obtained by linear interpolation.*[67]*

Similar as the vertical still water bending moment, there is no clear requirement from $IACS$ rule for shear force. It is also defined as case dependent issue.

2.5.4 Vertical wave shear force

DNV-GL rule

According to DNV-GL*[67]*, the vertical wave shear force at any longitudinal position is ruled in kN as:

Positive condition:

$$Q_{WV-pos} = 0.52 f_{q-pos} f_p C_W L B C_B \tag{40}$$

Negative condition:

$$Q_{WV-neg} = -(0.52 f_{q-neg} f_p C_W L B C_B) \tag{41}$$

where:

f_{q-pos} and f_{q-neg} are the distribution factors along the ship length for positive condition and negative condition illustrated in Figure 28 and Figure 29 respectively*[67]*.

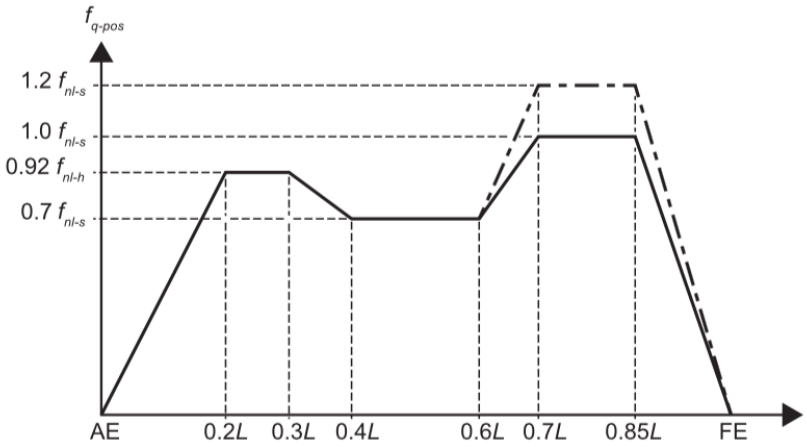

Figure 28: Distribution factor of positive vertical shear force f_{q-pos} defined by DNV (solid line).*[67]*

IACS rule

According to IACS rule, the wave shear force, F_W, in kN, at each section along the ship length are given by the following formula*[70]*:

For positive shear force:

$$F_W(+) = +30 F_1 \cdot C \cdot L \cdot B(C_B + 0.7) \times 10^{-2} \tag{42}$$

For negative shear force:

$$F_W(-) = -30 F_2 \cdot C \cdot L \cdot B(C_B + 0.7) \times 10^{-2} \tag{43}$$

where: F_1 and F_2 are the distribution factors given in Figure 30 and Figure 31 respectively*[70]*.

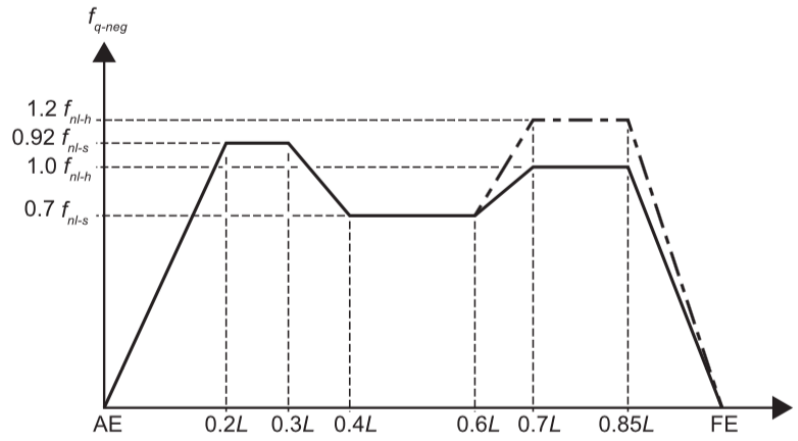

Figure 29: Distribution factor of negative vertical shear force f_{q-neg} defined by DNV (solid line).*[67]*

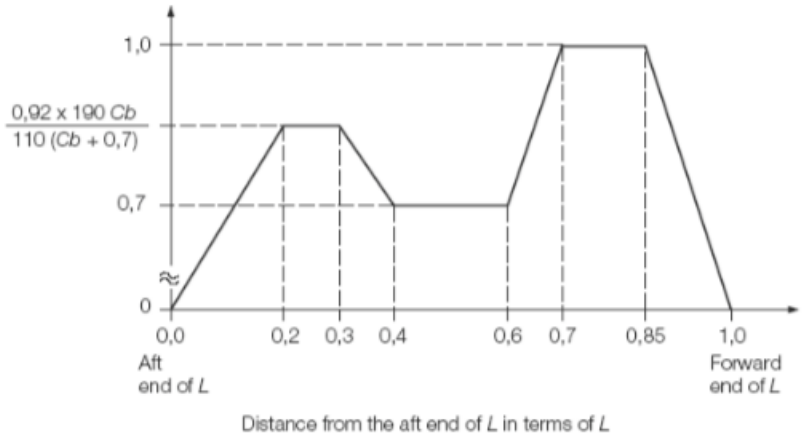

Figure 30: Distribution factor F_1 defined by DNV-GL.*[70]*

Comparing the vertical wave shear force requirement from DNV-GL in Equ. 40 and Equ. 41 and IACS in Equ. 42 and Equ. 43, a difference can be noticed. The extent of the difference depends on the value of block coefficient C_B. By calculation, it can be obtained:

For $C_B < 0.92$, IACS rule has lower standard in positive condition but higher requirement for negative condition than DNV-GL rule.

For $C_B = 0.92$, IACS rule and DNV-GL rule match with each other. The requirements are the same.

For $C_B > 0.92$, IACS rule has higher standard in positive condition but lower requirement for negative condition than DNV-GL rule.

Akira et al.*[72]* did a comparison between the IACS rule requirement in vertical wave shear force and that of 10 ship class societies. It is reported that the IACS rule

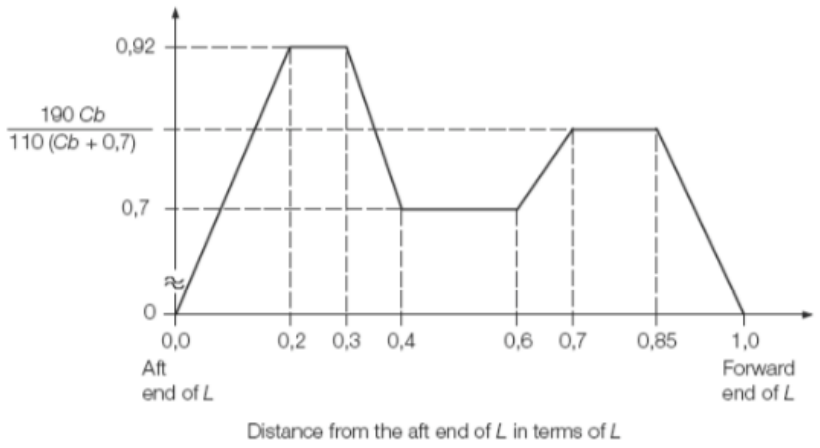

Figure 31: Distribution factor F_2 defined by DNV-GL.*[70]*

has higher requirement than the mean value of all. The likelihood level concerned by IACS is at 10^{-8}. The requirement of DNV-GL has the same level, but apparently, they have slight difference in the established rule.

2.6 Application process

The aim of the work is to find out the critical load that a commerical ship could meet and check the vertical bending moment and shear force under that circumstance. An indication of how the ship response shall be calculated with *strip method* is illustrated in Figure 32.

The steps for the application is listed as follow:

- Define the wave spectrums according to the wave statistics for all the possible wave conditions in terms of $H_{1/3}$ and T_z within its service area. This process is to be done with *Matlab*.
- Determine the vertical bending moment transfer funcitons for the model ship. The ship hull is to be created in *Napa*. The loading condition is to be defined. Reasonable strips shall be defined to describe the ship and the transfer functions are to be derived in the service speed V and several sailing directions μ. The transfer functions are to be transferred to *Matlab* for the response calculation.
- Multiply the wave spectrum with the transfer function squared according to Equ. 29. The transfer function for each direction shall be multiplied with each wave spectrum seperately and the largest amplitude of vertical bending moment shall be selected as soon as the responses are calculated. The relative wave condition and wave direction shall be captured. This process is done in *Matlab*.
- Check the vertical bending moment and shear force along the ship in the case sailing in the captured worst situation. Both hogging and sagging conditions are to be derived. The data are to be collected to *Matlab* again.

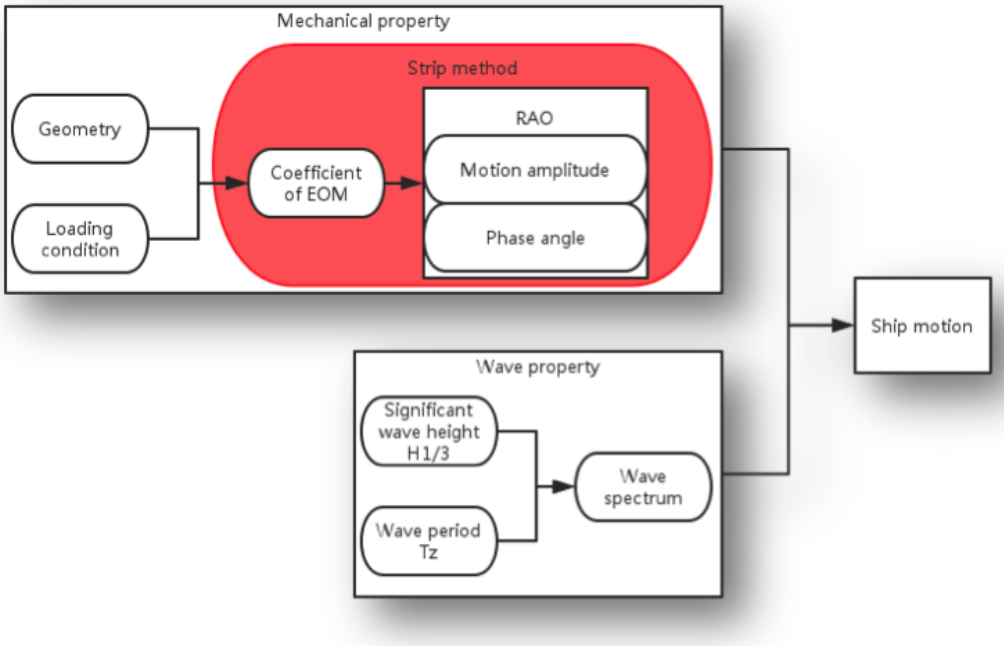

Figure 32: Ship motion calculation process with *strip method*.

– Compare the calculated results with the limitation ruled by DNV-GL rule and IACS rule. This process is done in *Napa*.

3 Result

3.1 Wave spectrum

As mentioned in the last section, for ship working in unlimited service area, North Atlantic Sea is usually assigned as the condition that should be modeled in the design stage. Table 7 is the scatter wave statistic chart that indicates the wave condition in North Atlantic Sea (Area 9) for all directions. The zero crossing period is counted with the interval of $1s$ and the significant wave height has the inverval as $1m$. In total, 1000 significant wave heights are captured and assigned in the table.

Table 7: Wave statistics for Area 9 in all directions according to Hogben et al (1986). *[64]*

ALL DIRECTIONS

PERCENTAGE OF OBS = 100.00%
(INCLUDING 1.95% DIRECTION UNKNOWN)

SIGNIFICANT WAVE HEIGHT (m)	<4	4–5	5–6	6–7	7–8	8–9	9–10	10–11	11–12	12–13	>13	TOTAL
>14	-	-	-	-	-	-	-	-	-	-	-	1
13–14	-	-	-	-	-	-	-	-	-	-	-	1
12–13	-	-	-	-	-	-	-	-	-	-	-	1
11–12	-	-	-	-	-	-	-	1	-	-	-	2
10–11	-	-	-	-	-	-	1	1	1	-	-	3
9–10	-	-	-	-	-	1	2	2	1	1	-	6
8–9	-	-	-	-	1	2	3	3	2	1	-	11
7–8	-	-	-	-	1	4	6	5	3	1	-	21
6–7	-	-	-	1	3	9	12	9	4	2	1	40
5–6	-	-	-	1	9	20	22	15	6	2	1	76
4–5	-	-	-	4	21	40	37	21	8	2	-	133
3–4	-	-	1	12	45	67	50	22	7	2	-	205
2–3	-	-	3	28	75	80	45	15	4	1	-	251
1–2	-	-	9	48	73	48	17	4	1	-	-	200
0–1	-	2	11	20	13	4	1	-	-	-	-	51
TOTAL	-	2	25	113	241	275	196	97	36	11	4	1000

ZERO CROSSING PERIOD (s)

Based on the scatter table, the ISSC wave spectrum formula (Equ. 9) is then modeled. The wave scatter chart are transferred into the wave spectrum $S_\zeta(\omega)$ as indicated in Figure 33. In Figure 33, each of the curve represents a wave condition with one wave height and one zero crossing period. The curves refer to the significant wave height H_z from $0.5m$ to $14.5m$ with the interval $1m$ and zero crossing period T_z from $3.5s$ to $13.5s$ with the interval $1s$. Here, $15 \times 11 = 165$ curves are generated.

However, not all the curves do exist. According to Table 3, the link of wave parameters in deep waters are indicated. The relationship between *mean crossing period* T_z and *wavelength* λ is also indicated as Equ. 44. Based on Equ. 44, the *wavelength* λ can be calculated referring to the *mean crossing period* T_z.

$$\lambda = \frac{gT_z^2}{2\pi} \tag{44}$$

As mentioned in the last section, the wave being studied is assumed to be *Stokes wave*, whose steepness is limited to be no more than 1/7. By checking the data in Table 7, it is also obvious that not all the wave spectrums plotted in Figure 33 really exist. Thus, those unreal wave spectrums are to be removed and the rest are plotted in Figure 34 and the valid wave spectrum is obtained.

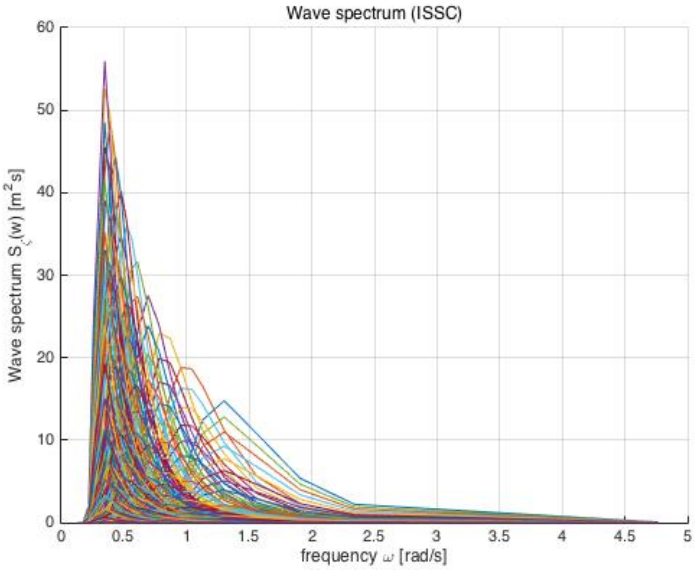

Figure 33: Wave spectrum in North Atlantic Sea according to ISSC rule referring to all the *significant wave height* and *zero crossing period*.

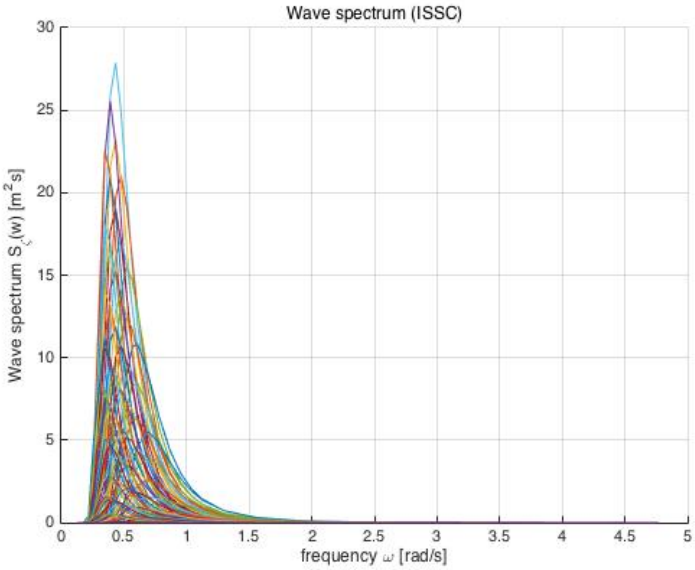

Figure 34: Wave spectrum in North Atlantic Sea according to ISSC rule referring to valid *significant wave height* and *zero crossing period* pairs.

3.2 Model ship

In the application of this thesis project, a general cargo ship called "*Napastar*" is selected as the model ship. The motivation of this selection is based on some reasons.

First of all, general cargo ships are very popular in transportation. According to a study in the seaborne trade shown in Figure 35, the transportation done by

general cargo ship occupied a majority proportion in 2014. It is reasonable to select a popular ship type to study.

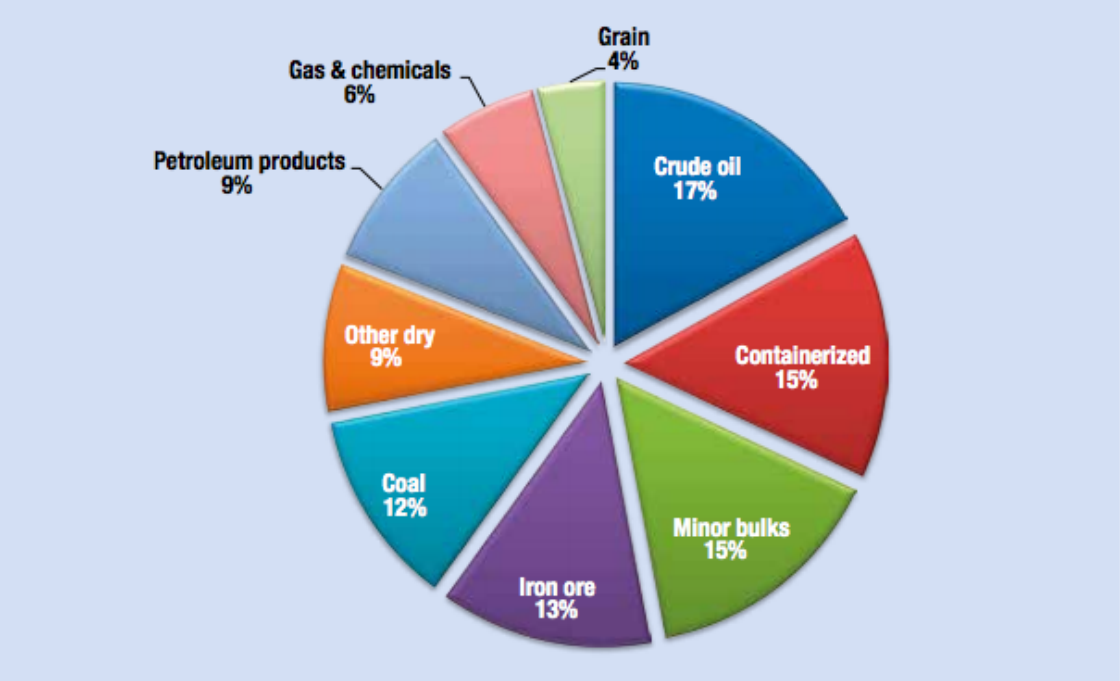

Figure 35: Structure of international seaborne trade, 2014(source: UNCTAD secretariat, based on Clarksons Research, Seaborne Trade Monitor, 2(5), May 2015).

Secondly, the DNV-GL rule and IACS rule in the vertical bending moment and shear force are more general for the general cargo ships. The vertial bending moment and shear force are most critical for general cargo ship, but for other ships, there are always other additional requirements. For example, for container ships, the tortional strength is usually more critical due to big openings on deck. It is wise to select the ship type, for which the vertical bending moment and shear force are crucial.

Thirdly, to apply the *strip method*, there are some assumptions and limitations. For instance, the operation speed should be relatively low and the motions are assumed to be small. A full load general cargo ship fulfills those assumptions best. The validation of the method applied in the thesis work is important to be guaranteed.

Further more, *Napa* is employed for the ship mechanical property calculation. The model of *Napastar* exists in the database of *Napa*. The existing model reduces the working load in model definition and efforts can be put on the study in hull girder loads. Besides, a relative mature model is more stable and less mistakes are expected in the calculation.

Based on all those reasons, the model ship *Napastar* is decided to be used for this thesis project study.

3.2.1 Ship parameter and drawings

The model ship *Napastar* is a general cargo ship with two cargo holds. The machinery room and superstructure are located at the stern of the ship. It is operated by one propeller and a rudder. The service speed V is 15 knots, and the service area is unlimited. The main parameters of *Napastar* is listed in Table 8 and a rough image of its 3D-model is shown in Figure 36. The general drawing of the ship and more details about the parameters are illustrated in Appendix A.

Table 8: Main parameters of *Napastar*.

Length, overall	L_{OA}	$= 90$	m
Length, waterline	L_{wl}	$= 84.3$	m
Length between perpendiculars	L_{pp}	$= 82$	m
Beam, waterline	B_{wl}	$= 13$	m
Beam, maximum	B_{wl}	$= 13$	m
Draught	T	$= 4.88$	m
Displacement volume	D_{isv}	$= 4331$	m^3
Block coefficient	C_B	$= 0.8323$	

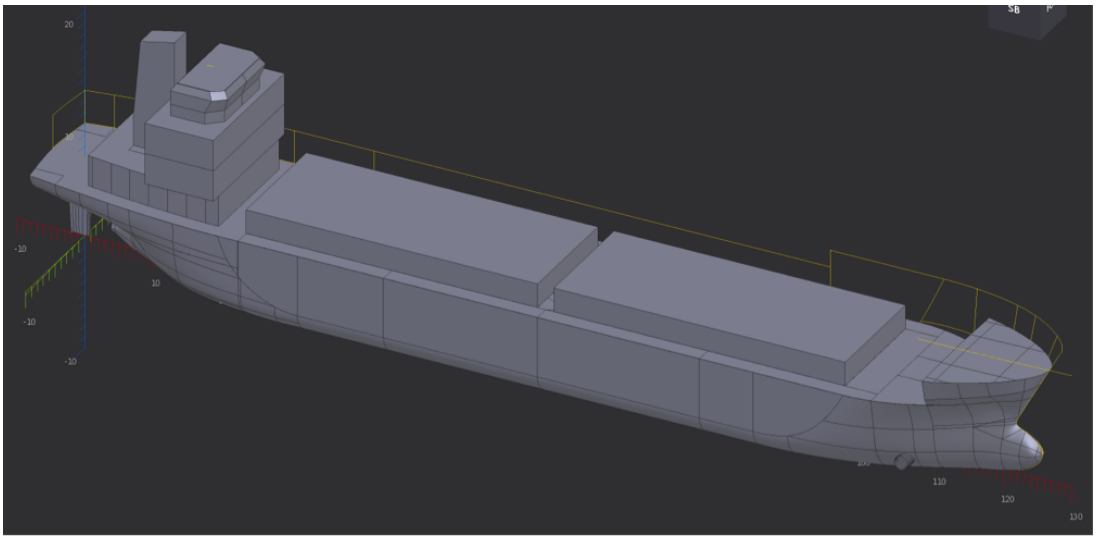

Figure 36: The 3D model of *Napastar*.

3.2.2 Loading condition

Every ship has its mission. For *Napastar*, the mission is to transport cargoes from one port to another. Thus, there are conditions such as staying in port, operating with cargoes and without cargoes. They can be described as four loading conditions:

– Bare ship, with just lightweight structures.

– Ballast condition, with no cargo inside but ballast water for stability.

– Half loading condition, with part of the cargo holds filled with cargoes.

– Full loading condition, with all the cargo holds full, but empty in ballast tanks.

Among them, the full loading condition is chosen as the study object, since DNV-GL rule and IACS rule have their requirement in this loading condition. The full loading condition is illustrated in Appendix B in Figure B1 with all the detailed tank filling information listed in Table B1. It can be seen in that the cargo holds are full of cargoes but no ballast in any tank. Under the floating position gives the ship parameters in the full loading condition which is illustrated in Table B2 and the weight distribution is illustrated in Figure 37.

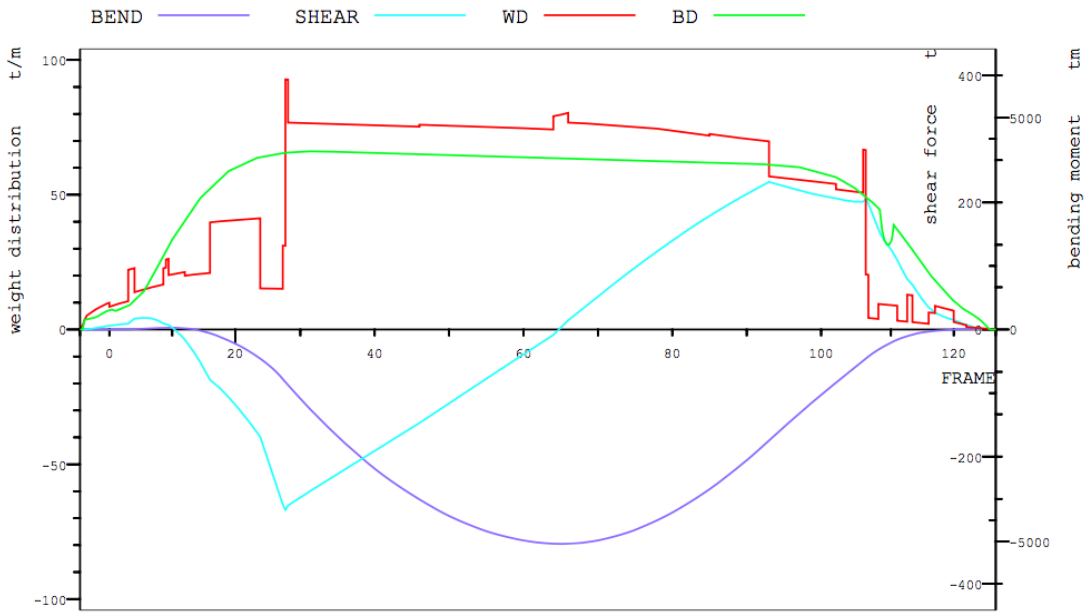

Figure 37: Weight distribution, buoyancy distribution, vertical bending moment and shear force along the stationary ship under full loading condition in still water.

3.2.3 Input for strip method

To apply the strip method, the ship is decribed by 20 sectional strips. The division of the strips is listed Table C1 in Appendix C, where $Frxcor$ is the X-coordinate of sections over ship length with the original point at CoG. Frx is the absolute X-coordinate in *meter* but with the original point at stern. The others are coefficients related to the *Lewis transform*.

The defined regular waves are indicated in Table C2. In Table C2, it can be seen that the relationship between the wavelength λ (in appendix W_{Len}) and the

zero crossing period T_z (in appendix H_z) follows Equ. 44. That is because the water depth is set as $10000m$ which is deep. The density of sea water is defined as $\rho = 1025kg/m^3$.

In reality, the ship will need to face the wave from any directions. In the application, the ship is assumed to be sailing in eight directions. They are the head sea $\mu = 180^o$, bow sea $\mu = 135^o, 235^o$, beam sea $\mu = 90^o, 270^o$, quartering sea $\mu = 45^o, 315^o$ and following sea $\mu = 0^o$. Since the geometry of the ship is symmetric, the five of them are taken for calcuation so as to avoid repeating work. A notion of the five directions are indicated in Figure 38. The input speed is assigned to be at the service speed, $V = 15knot$, Froude number $Fn = 0.268$.

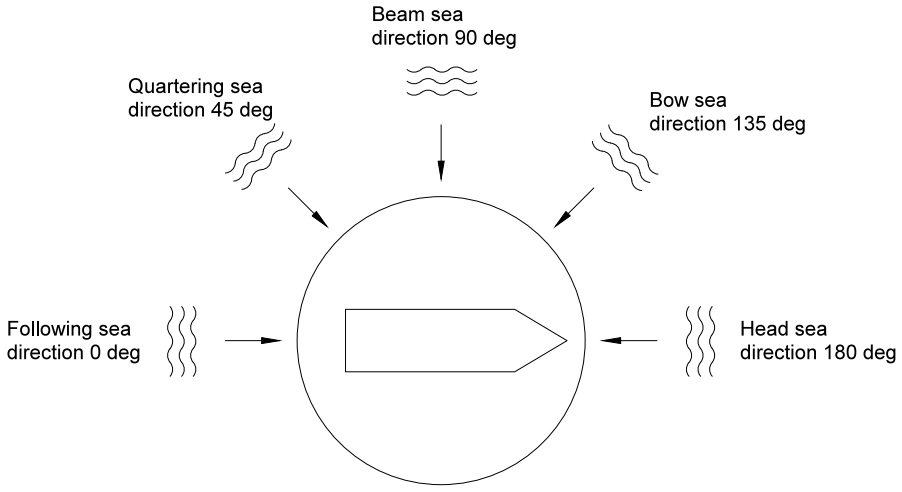

Figure 38: Notion of different wave directions.

3.3 Transfer function of vertical bending moment

By applying strip method in *Napa Seakeeping* module and transfer the data to *Matlab*, the transfer function of vertical bending moment is plotted in Figure 39. The transfer function $Y(\omega)$ is taken under full loading condition and the service speed ($V = 15knot$) and non-dimensionalized by ($\rho \cdot g \cdot B \cdot L_{pp} \cdot \zeta$). Each curve represents the transfer function in one sailing direction from 0 to 90^o. This non-dimensionalization tells the nonlinear level which *Napa* achieves that the hydrostatic pressure over the wetted hull surface is related to the elevation of water surface.

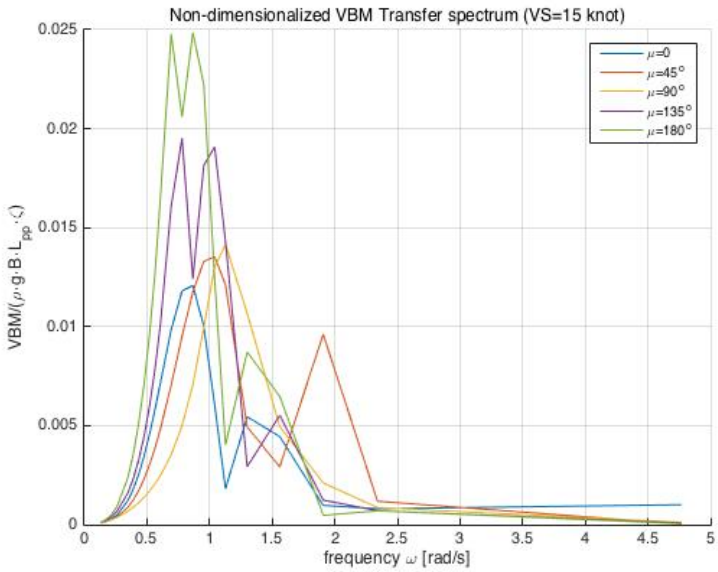

Figure 39: non-dimensionalized vertical bending moment transfer function V=15 knots. The transfer function is non-dimensionalized by $(\rho \cdot g \cdot B \cdot L_{pp} \cdot \zeta\ )$

3.4 Ship response of vertical bending moment

Now, both of the wave spectrum $S_\zeta(\omega)$ and the transfer function $Y(\omega)$ of vertical bending moment are obtained. According to Equ. 29, the response function $S_\eta(\omega)$ of vertical bending moment shall be calculated and plotted in Figure 40.

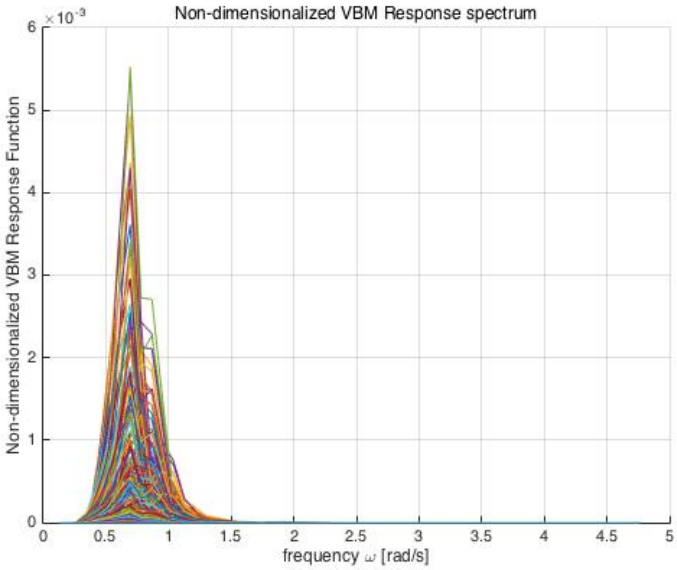

Figure 40: Non-dimensionalized vertical bending moment response function V=15 knots.

With the response function, the variance σ_η^2 and the standard deviation σ_η can be

calculated according to Equ. 31, which represents the amplitude of vetical bending moment. Hence, by comparing the standard deviation, the most critical sea states can be locked. To avoid the inaccuracy of the integration in Equ. 31, which could lead to inaccurate rank of σ_η^2, the first five critical sea states are presented in Table 9 instead of just one.

Table 9: Coefficients for different variants of ISSC and ITTC wave spectrum. $H_{1/3}$ is the significant wave height and T_z is the mean zero crossing period.

H_z[m]	T_z[s]	λ[m]	$\sigma_\eta^2 \times 10^{-3}$	μ^o
9.5	8.5	113	1.378	180
8.5	7.5	88	1.370	180
10.5	9.5	141	1.305	180
11.5	10.5	172	1.198	180
8.5	8.5	113	1.103	180

In Table 9, the first two columns are the significant wave height H_z and the zero crossing period T_z, which directly refer to the wave scatter chart in Table 7. The third column is the wavelength λ calculated with T_z according to Equ. 44. The fourth column is the variation devived from response function. The last column is the sailing direction referring to the curve in transfer function.

3.5 Vertical bending moment along the ship

The dynamic vertical bending moment can be divided into two parts, the still water VBM and the wave VBM. The former is the static load and by summing them up, the dynamic load can be derived. Here, the results of VBM is to be presented in three forms, the static VBM (still VBM), the wave VBM and the dynamic VBM.

The static VBM, which is also the still water VBM of *Napastar* is illustrated in Figure 41. In Figure 41, the x-axes is the distance from stern to bow, with the entire length defined in *S2[69]*. The y-axes is the vertical bending moment in kNm. The wide polylines in blue and red represent the DNV-GL rule requirement in still water VBM according to Equ. 32 and Equ. 33. The yellow narrow curve is the calculated still water VBM under full loading condition, and the purple narrow curve is the calculated still water VBM under 140% full loading condition. The 40% loading is applied in the cargo hold, with extra 40% cargoes or 40% increasing in cargo density.

In Figure 42, the vertical wave bending moment along the ship with respect to various waves is illustrated. The x-axes is the distance from stern to bow, with the entire length defined in *S2[69]*. The y-axes is the vertical bending moment in kNm. The wide dashed polylines in black represent the calculaiton results according to the DNV-GL rule in water VBM with Equ. 34 and Equ. 35. The wide dashed polylines in black represent the calculation results according to the IACS rule in water VBM

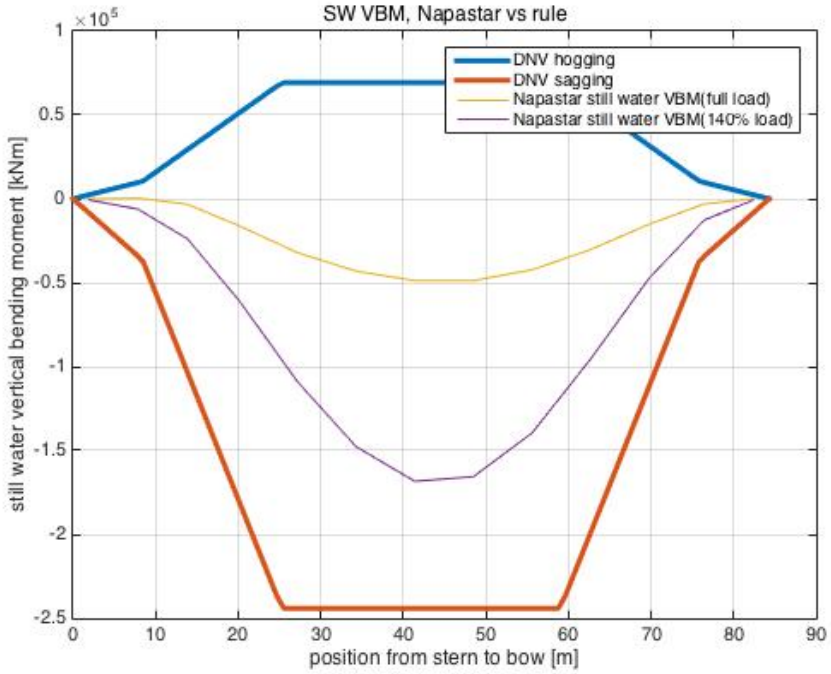

Figure 41: Still water (static) vertical bending moment, *Napastar* vs rule.

with Equ. 36 and Equ. 37. As mentioned in in Section 2, DNV-GL and IACS have the same requirement for the wave VBM. The curves in various colors represent the calculated results with the waveS indicated in Table 9. Among them the wide dotted curve in blue is derived with the wave parameter $H_z = 8.5m$, $T_z = 7.5s$, $\lambda = 88m$.

By combining the still water VBM and the wave VBM, the dynamic VBM requirement of DNV-GL and IACS can be derived and illustrated in Figure 43. The x-axes is the distance from stern to bow in m, with the entire length defined in *S2[69]*. The y-axes is the vertical bending moment in kNm. The wide dashed polylines in black represent the DNV-GL rule requirement in dynamic VBM according to the combination of Equ. 34 with Equ. 34 and Equ. 33 with Equ. 35. For IACS rule, the still water VBM is not clearly ruled in formula. Here the still water VBM from DNV-GL rule is added with the wave VBM ruled by IACS to present the dynamic VBM. Since the DNV-GL rule and IACS rule have the same requirement for the wave VBM, by adding the same still water VBM, the same dynamic VMB is obtained. The curves in various colors represent the calculated results with the wave indicated in Table 9. Among them, the wide dotted curve in blue, which is the most critical one, is derived with the wave parameter $H_z = 8.5m$, $T_z = 7.5s$, $\lambda = 88m$. Besides, an extra green curve is plotted with the wide dash-dot, which is derived with the wave parameter $H_z = 7.5m$, $T_z = 7.5s$, $\lambda = 88m$.

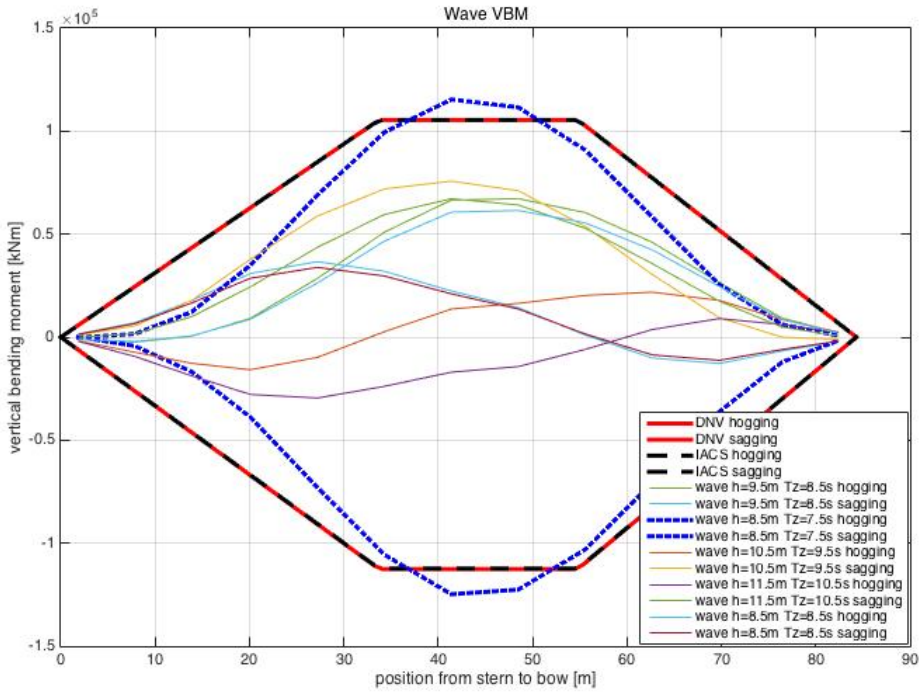

Figure 42: Wave vertical bending moment, *Napastar* vs rule.

3.6 Shear force along the ship

Similar as the dynamic vertical bending moment, the dynamic vertical shear force along the ship is also composed by the still water VSF and wave VSF. The results from calculation and the rule requirements are illustrated here in the three forms.

The static vertical shear force, which is also the still water vertical shear force of *Napastar* is illustrated in Figure 44. In Figure 44, the x-axes is the distance from stern to bow, with the entire length in m, defined in *S2[69]*. The y-axes is the vertical shear force in kN. The wide polylines in blue and red represent the DNV-GL rule requirement in still water VSF according to Equ. 38 and Equ. 39. The yellow narrow curve is the calculated still water VSF of *Napastar*, and the purple narrow curve is the calculated still water VSF under 140% full loading condition. The 40% loading is applied in the cargo hold, with extra 40% cargoes or 40% increasing in cargo density.

In Figure 45, the wave vertical shear force along the ship with respect to various waves is illustrated. The x-axes is the distance from stern to bow in m, with the entire length defined in *S2[69]*. The y-axes is the vertical shear force in kN. The wide dashed polylines in black represent the calculaiton results according to DNV-GL rule in wave VSF with Equ. 28 and Equ. 29. The wide dashed polylines in black represent the calculation results according to the IACS rule in water VSF with Equ. 42 and Equ. 43. Not like the wave VBM that DNV-GL and IACS have the same formula for calculation, but they give different formula for negative wave VSF. The

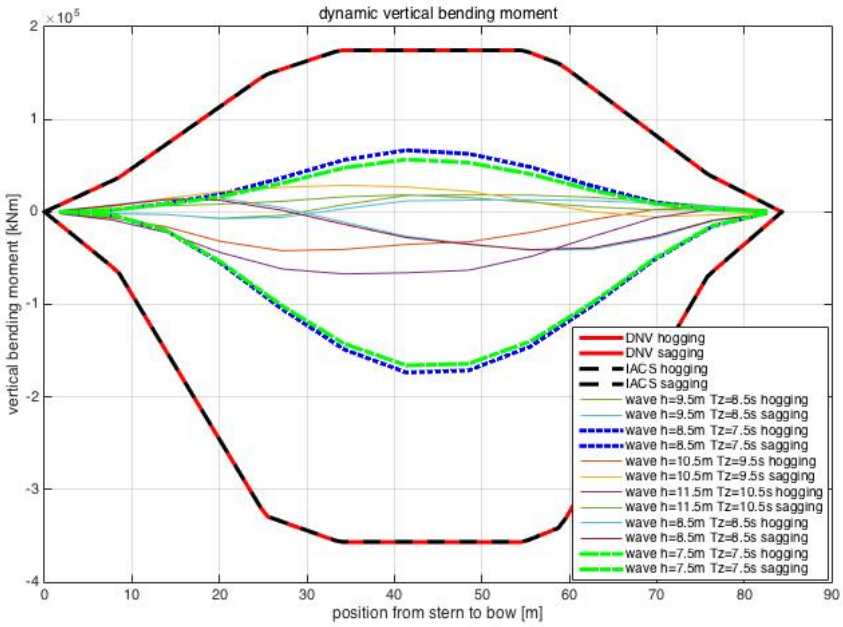

Figure 43: Dynamic vertical bending moment, *Napastar* vs rule.

curves in various colors represent the calculated results with the wave indicated in Table 9. Among them the wide dotted curve in blue is derived with the wave parameter $H_z = 8.5m$, $T_z = 7.5s$, $\lambda = 88m$.

Meanwhile, the wave VSF, $Q = Q_{napa}$ derive by *Napa* and the calculated one $Q_{cal} = dM/dt$ is plotted in Figure 46. In the figure, the x-axes is the distance from stern to bow in m, with the entire length defined in *S2[69]*. The y-axes is the vertical shear force in kN. The wide dashed polylines in black represent the calculaiton results according to DNV-GL rule in wave VSF with Equ. 28 and Equ. 29. The wide dashed polylines in black represent the calculation results according to the IACS rule in water VSF with Equ. 42 and Equ. 43. The curve in blue represents Q_{napa} and the curve in green is derived by $Q_{cal} = dM/dt$.

By combining the still water VSF and the wave VSF, the dynamic VSF requirement of DNV-GL and IACS can be derived and illustrated in Figure 47. The x-axes is the distance from stern to bow in m, with the entire length defined in *S2[69]*. The y-axes is the vertical shear force in kN. The wide dashed polylines in black represent the DNV-GL rule requirement in dynamic VSF according to the combination of Equ. 38 with Equ. 39 and Equ. 28 with Equ. 29. Again, for IACS rule, the still water VSF is not clearly ruled in formula. Here the still water VSF from DNV-GL rule is added with the wave VSF ruled by IACS to present the dynamic VSF. The curves in various colors represent the calculated results with the wave indicated in Table 9. Among them, the wide dotted curve in blue, which is the most critical one, is derived with the wave parameter $H_z = 8.5m$, $T_z = 7.5s$, $\lambda = 88m$. Besides, an extra green curve is plotted with the wide dash-dot, which is derived with the wave parameter $H_z = 7.5m$, $T_z = 7.5s$, $\lambda = 88m$.

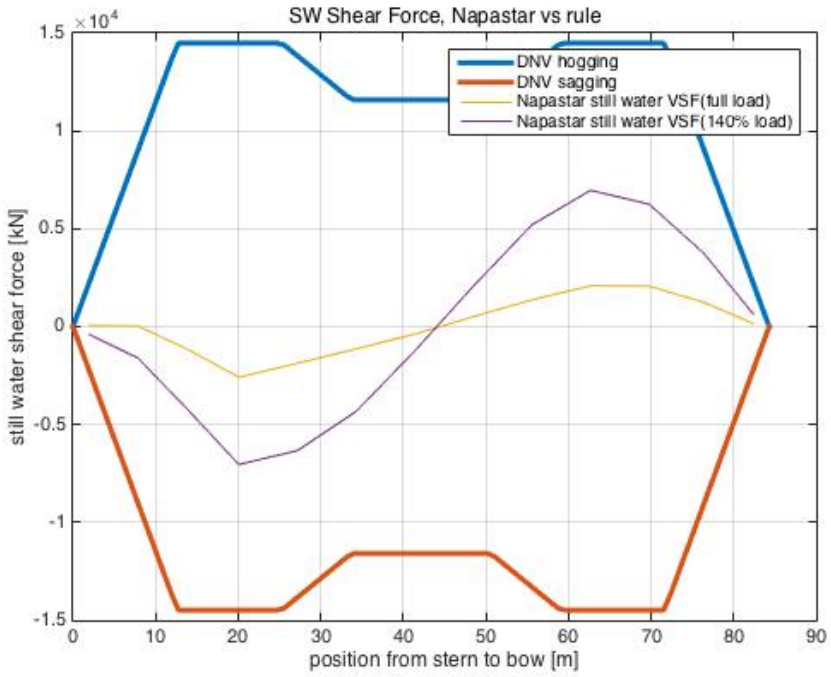

Figure 44: Vertical still water shear force, *Napastar* vs rule.

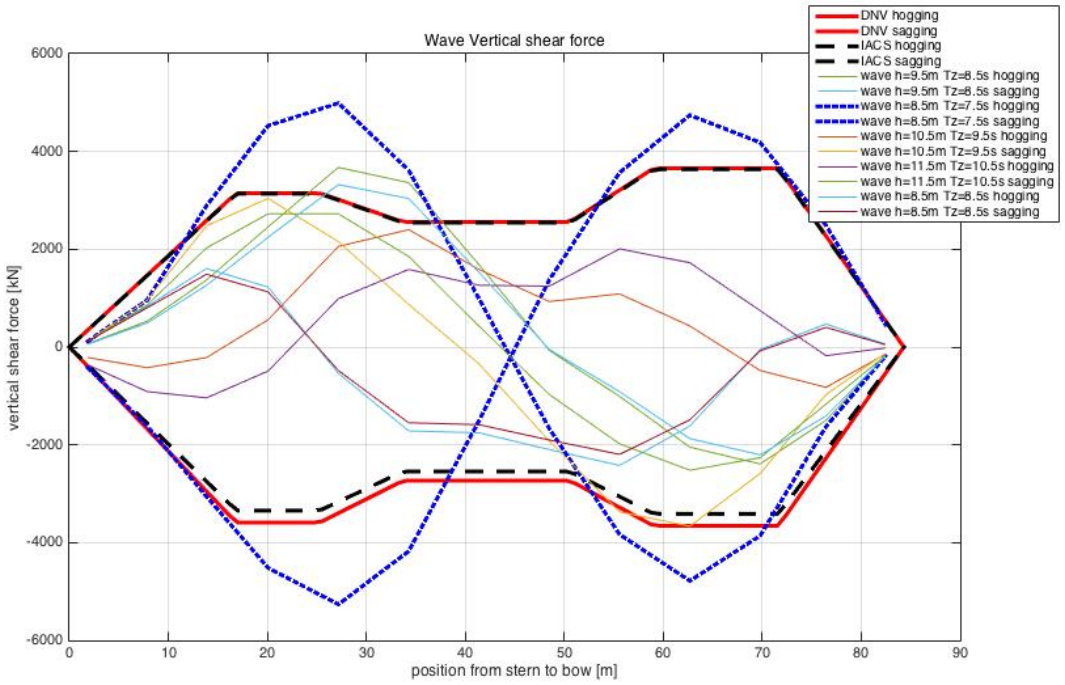

Figure 45: Vertical wave shear force, *Napastar* vs rule.

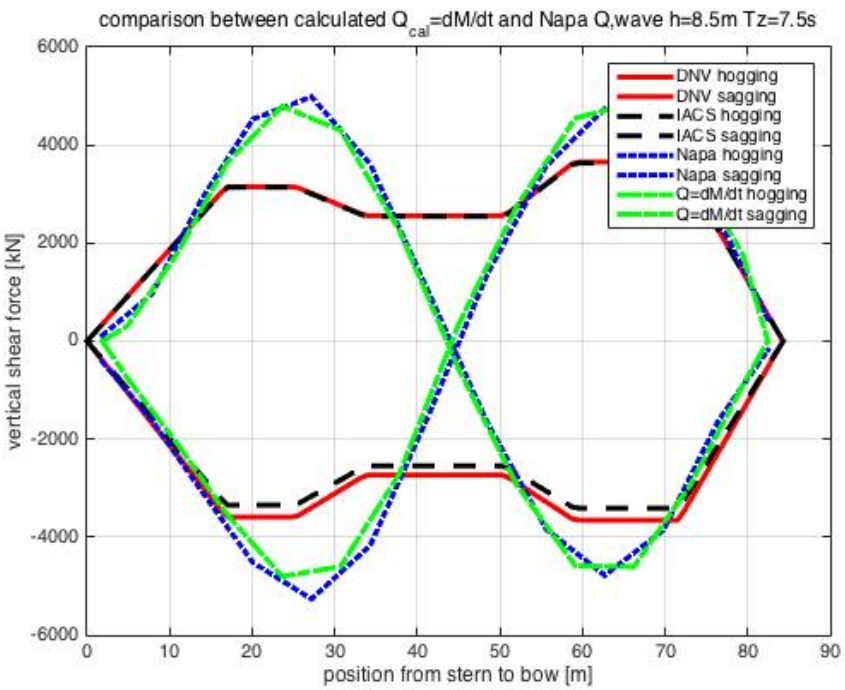

Figure 46: Vertical wave shear force, derived by $Napa$ vs dervied according to dM/dt, with wave parameter $H_z = 8.5m$, $T_z = 7.5s$.

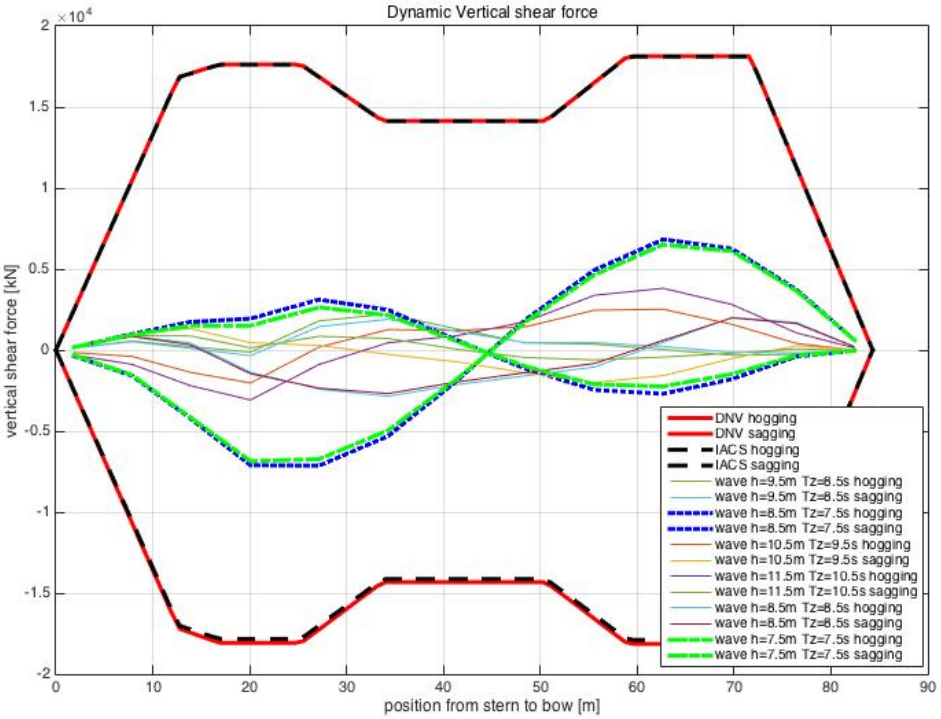

Figure 47: Dynamic vertical shear force, $Napastar$ vs rule.

4 Discussion

The target of the thesis work is to suggest a feasible method for loads on hull girders in the preliminary design stage. With all the results plotted, it is time to go back for the targeted questions, which mentioned in sub-section 1.4. Besides, some additional information is indicated in the results. The factors relating to the loads shall also be discussed.

4.1 Validation of DNV-GL rule and IASC rule

According to DNV-GL rule*[67]* and IACS rule*[70]*, there are requirement for the loads on hull girders. The clarification in the rules indicates the requirement for the *static loads* and the *dynamic loads*. The *static loads* are the same as *still water loads*. In addition to them, together with the the *wave loads*, the *dynamic loads* are to be determined. To make it clear, the *wave loads* are not ruled by DNV-GL or IACS, but only the *static loads* and the *dynamic loads*. Here, the loads in those three kinds shall be discussed separately so as to judge the validation of rule requirement.

4.1.1 Static vertical loads

The DNV-GL rule for the still water vertical bending moment is illustrated in Figure 41 and compared with the calculated result. It can be seen, the calculated result is from 0 on the bow side and stern side to -0.5×10^5 kNm in the middle, while the upper limit of the rule is about 0.7×10^5 kNm and the lower limit is around -2.5×10^5 kNm in the middle. There, the nonlinearity is obtained.

Under the full loading condition, the ship has a downward bending moment -4.9×10^4 kNm. Comparing the calculated VBM and the rule, a big margin can be obtained. Thus, regarding the still water VBM, *Napastar* should be able to carry more cargoes. According to the design, the cargo hold is filled with the cargo which has a density at $1000kg/m^3$. To understand the bound of the rule, the 40% extra cargo is filled into the cargo hold, and the still water VBM turns out to be -1.7×10^5 kNm. It is expected that as soon as 180% is filled, the still water VBM will reach the bound of rules.

The DNV-GL rule for the still water vertical shear force is illustrated in Figure 44, together with the calculated result of *Napastar*. The rule requirement is derived according to Equ. 38 and Equ. 39. It can be seen that the still water VSF has the same value for positive condition and negative condition but of the opposite directions. Similar as the still water VBM, the still water VSF is plotted for the full loading condition and 140% loading condition. They are both within the range of the rule, but if the loading condition is increased to 200%, the shear force is about to touch the bound of rules.

The DNV-GL rule in still water VBM and VSF are not fixed number for all the ships, but closely related to the size of the ship. Ships with larger longditudinal size usually have relative higher still water VBM and VSF, and the requirement is reasonably higher with respect to the ship size.

In this case, for both the still water VBM and VSF, a large tolerance between the DNV-GL ruled amount and the calcuated results is obatined for the ship under full loading condition. Though under a doubled cargo amount is about to touch the bound of the rules, there is the doubt if there is an overestimation in both VBM and VSF for the DNV-GL rule requirement.

4.1.2 Wave vertical loads

As illustrated in Figure 42 and comparing Equ. 34 and Equ. 35 with Equ. 36 and Equ. 37, the wave VBM requirement from the two associations are the same. Comparing the requirement for the hogging condition and the sagging condition, the nonlinearity is obvious in Figure 42. The difference of the wave VBM in hogging and sagging conditions is closely related to the block coefficient C_B as indicated in Equ. 45. The ratio of hogging to sagging wave VBM M_{WV-h}/M_{WV-s} is shown in Figure 48.

$$\frac{|M_{WV-h}|}{|M_{WV-s}|} = \frac{1.73C_B}{C_B + 0.7} \tag{45}$$

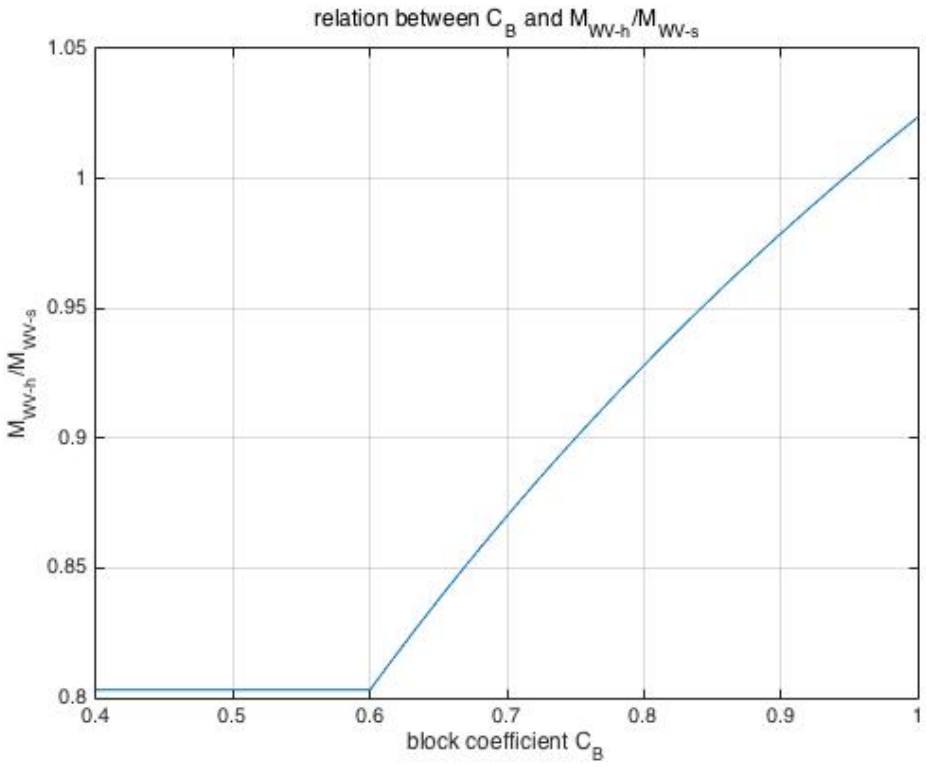

Figure 48: Relation between block coefficient C_B and the ratio of hogging to sagging wave vertical bending moment M_{WV-h}/M_{WV-s}

According to Akira et al.*[72]*, GL'86 Rule, BV'86 Rule and DNV'88 Rule gave constant nonlinear requirement between hogging and sagging conditions. The ratio

of hogging to sagging VBM M_{WV-h}/M_{WV-s} was considered no relation with the block coefficient C_B, and it was about 0.9 for any block coefficient. Apperently, the IACS rule and nowadays DNV-GL rule give more concern in the nonlinearity. There is more difference between the hogging and sagging wave VBM requirement when the block coefficient is smaller.

As illustrated in Figure 42, the ratio of hogging to sagging VBM according to the rule is $M_{WV-h}/M_{WV-s} = 0.94$. The calculated results give the ratio of hogging to sagging VBM is $|M_{WV-h}|/|M_{WV-s}| = 0.93$, for the most critical wave state. It is almost the same as required by the rules. Besides, the trend of the calculated curve fits the rule requirement well. However, neither the hogging wave VBM nor the sagging wave VBM is within the rule requirement range. Although it is very close to the rule bound, there is underestimation in the ruled wave VBM.

For the wave VSF, DNV-GL and IACS give the same requirement for the positive condition but different ones for the negative condition. Seen from Figure 45, by binding the nonlinearity of wave VBM with that of wave VSF, Equ. 46 can be derived. It tells the effect of the nonlinearity in wave VSF considered by IACS is even as that of the wave VBM. The DNV-GL rule is also very close to the IACS rule.

$$\frac{|F_W(+)_2|}{|F_W(-)_2|} = \frac{|F_W(-)_7|}{|F_W(+)_7|} = \frac{|M_W(+)_{mid}|}{|M_W(-)_{mid}|} \tag{46}$$

Comparing the calculated results with the wave parameter $H_z = 8.5m$, $T_z = 7.5s$, $\lambda = 88m$ and the rule wave VSF requirements indicated in Figure 45, the trend of the calculated curves fit well with the rules, and the effect of nonlinearity is very close. However, there are some cases whose shear force exceed the range of rule requirement. Similar as the wave VBM, there could be an underestimation in both DNV-GL rule and IACS rule for wave VSF.

4.1.3 Dynamic vertical loads

By adding the static vertical loads and wave vertical loads, the dynamic vertical loads can thus be derived. In Figure 43, the dynamic VBM is shown. Since the static VBM and wave VBM are the same for DNV-GL rule and IACS rule, the dynamic VBM are also the same for them. The dynamic VBM required by rules have the trend that the largest bending moment is ruled in the middle of the ship and decreases to the bow and stern side. Inheritated from the still water VBM and wave VBM, the dynamic VBM also shows the effect of nonlinearity between hogging and sagging conditions. In this case, the hogging dynamic VBM in the middle is $M_{dy-h-mid} = 1.747 \times 10^5\ kNm$ and the sagging one is $M_{dy-s-mid} = -3.565 \times 10^5\ kNm$. The effect of nonlinearity can thus be presented as the ratio between them, which is $|M_{dy-h-mid}|/|M_{dy-s-mid}| = 0.49$.

Among the calculated results, the curve derived with the wave parameter $H_z = 8.5m$, $T_z = 7.5s$, $\lambda = 88m$, again, is the most critical one. It has the same trend as the rule requirement because the wavelength is very close to the ship length. It also shows most critical bending moment in the middle of the ship, which is

$M_{dy-h-mid-cal} = 6.662 \times 10^4\ kNm$ for hogging and $M_{dy-s-mid-cal} = -1.736 \times 10^5\ kNm$ for sagging. The ratio between them is $|M_{dy-h-mid-cal}|/|M_{dy-s-mid-cal}| = 0.38$, which shows a heavier effect of nonlinearity comparing with the rules.

Figure 43 also shows that all the results are within the ruled range. To take the critical result for comparison, in hogging condition, the limit of rule is 1.6 times higher than the calculated one, and in sagging condition, the rule limit doubles the calculated one. Since the calculated result is just from one case, it is not sufficient to represent all, but according to this case, the margin seems to be quite reasonable.

From Figure 47, it can be seen that similar as the wave VBM, the dynamic VBM rules from DNV-GL and IACS give very close requirement and the trend of the critical curve matches that of the rules. All the result curves are within the range of the rule quirement. However, according to the data indicated in Table 10 and Table 11, for the critical result, the nonlinearity is higher comparing with the rules. Besides, there is a margin between the rule requirement and the calculated results, the lowest at 61% and highest at 85%. Similar as the dynamic VBM, this margin could be reasonable, if considering other cases.

Table 10: Ruled dynamic vertical shear force at $0.25L$ and $0.7L$.

	$DNV-GL(+)$ $[kN]$	$IACS(+)$ $[kN]$	$DNV-GL(-)$ $[kN]$	$IACS(+)$ $[kN]$
$0.25L$	17620	17620	-18070	-17830
$0.7L$	18120	18120	-18140	-17890

Table 11: Calculated dynamic vertical shear force at $0.25L$ and $0.7L$ with the wave parameter $H_z = 8.5m$, $T_z = 7.5s$, $\lambda = 88m$.

	$Calculated(+)$ $[kN]$	$Calculated(-)$ $[kN]$	$Ratio$ $(+)/(-)$
$0.25L$	3116	-7134	0.44
$0.7L$	6831	-2695	2.53

4.2 Feasibility of Napa

The feasibility of Napa actually includes the whole calculation process that indicated in subsection 2.6. It can be judged by considering the accuracy and time consumption of the numerical calculation.

4.2.1 Accuracy

First of all, a comparison shall be done between the frequency-domain predicited critical waves with the waves which generate critical hull girder loads. Table 9 indicates the five most critical waves generated by the frequency-domain calculaiton. Among them, $wave_1$ with the parameter $H_z = 9.5m$, $T_z = 8.5s$, $\lambda = 113m$ is predicted to have the largest amplitude for the VBM. $wave_2$ with the parameter $H_z = 8.5m$, $T_z = 7.5s$, $\lambda = 88m$ is predicted to have the second largest amplitude for the VBM. However, in the dynamic VBM indicated in Figure 43, $wave_2$ is the most critical one, and the second critical wave is the one with the parameter $H_z = 7.5m$, $T_z = 7.5s$, $\lambda = 88m$, which is not even in the rank of Table 9. Actually, the amplitude is not able to describe the VBM completely. It just shows the potential maximum bending moment that the ship might face. The complete estimation of the VBM needs to generate the phase function as well. Despite this, the most critical wave condition is included in the rank of Table 9, which is suggested by the frequency-domain solution. Hence, the accuracy, in this manner, can be understood as reliable.

Secondly, the interval of recording the wave spectrum is subjective. This could lead to some inaccuracy in the prediction. Besides, the interval of requency ω may lead to the similar inaccuracy. For instance, the difference in suggesting the critical waves mentioned in the last paragraph could be due to this reason as well. The amplitude is the variance of integration of $Y_\eta(\omega)$ with the frequency ω. However, the interval is inevitable. As long as there is a motivation in selecting a reasonable interval, the accuracy should be acceptable. Of course, the smaller intervals are selected, the more accurate results can be derived, but it also costs more time in calculation.

Thirdly, this thesis project is done with *strip method*. the strip method is a quick method. It describe the ship in strips and solve the 3D problem with the 2D method. It is a rough description for the ship hull. Further more, when forming the shapes of strips, the *Lewis transform* is applied, which is also a convenient method in application but not so accurate. However, given that the model ship is qualified to apply the strip method, the accuracy can be accepted in an engineering point of view, especially for the priliminary design.

Comparing the wave VSF generated by *Napa* witht the one derived according to $Q = dM/dt$ shown in Figure 46, it can be seen that they give the same results. *Napa* agree with Equ. 27. In this manner, *Napa* is reliable.

The last but not the least, this thesis project is done in frequency-domain, and the level of nonlinearity taken into consideration is *Level* 2: $Froude - Krylov$ *nonlinear* according to the definition by ISSC*[4]*. The accuracy is for sure related to the level of nonlinearity. The higher level refers to higher accuracy. However, the frequency-domain solution is just suitable for *Level* 1 and *Level* 2, but for higher levels, only time-domain solution is applicable. The higher accuracy refers to longer time consumption. For the early stage design, to use the *Level* 2 of nonlinearity is adequate and clever, since it is the higher level that frequency-domain solution can be used.

4.2.2 Time consumption

The time consumption is defined as the time used by an adept engineer to go through the entire process and deliver all the results. With the scripts made in both *Napa* and *Matlab*, the computation can be done and the time consumption can be estimated. For *strip method*, the calculation time for transfer function is rather quick, which is about several seconds. The scripts in *Matlab* runs also fast in seconds. Most time is consumed to tranfer data from *Napa* to *Matlab*. Efforts have been put to generate the irregular wave response in *Napa*, but due to the unclearance of wave spectrum defination, the result is judged not reliable. The time including running the code and making the adjustment can be done in two days.

In summary, the time consumption is not a lot. The accuracy is quite acceptable for preliminary design. Hence, *Napa* is practical in use for the early ship design stage.

4.3 Factors influencing the loads on hull girder

In addition to the calculation method, the factors influencing the loads on hull girder can also be concluded from the calculation results. The experience in motivating critical wave condition and ship parameter would be useful to evaluate the application efficency. The factors include the wave parameters as well as the ship parameters. They are to be discussed separately.

4.3.1 Wave parameter

The main wave parameters include all the parameters shown in Table 3. The relationship between the parameters is also indicated in the table. As long as the problem is limited in deep sea, the relations are valid. Thus, for all those parameters, it is enough to focus on one of them. Here, the wavelength λ is to be discussed. Besides, the wave height H is an important parameter. With the two factors, the wave spectrum can be determined. Here, the wave steepness H/λ is to be discussed.

Wavelength
It is hard to judge if a wave has a long wavelength or a short or a short one without any reference. Usually, instead of the wavelength λ, the ratio of wavelength to ship length λ/L is better to discuss. An indication of the ratio is shown in Figure 49.

It can be imagined that if a wave has infinite wavelength, operating in that wave would have no difference as operating in calm water such as indicated in Figure 49 *a*). On the other hand, if the the ratio is very small, just like indicated in Figure 49 *b*), there would be no impact on the ship either, since the wave is always propagating. The largest excitation forces on ship appear when the wavelength λ is close to the ship length L, where $\lambda/H = 1$.

This can also be concluded by observing the wave VBM and wave VSF in Figure 42 and Figure 45. In the two figures, the wave condition with parameter $\lambda = 88m$ is the most critical one, comparing with the other curves with the same wave height. In

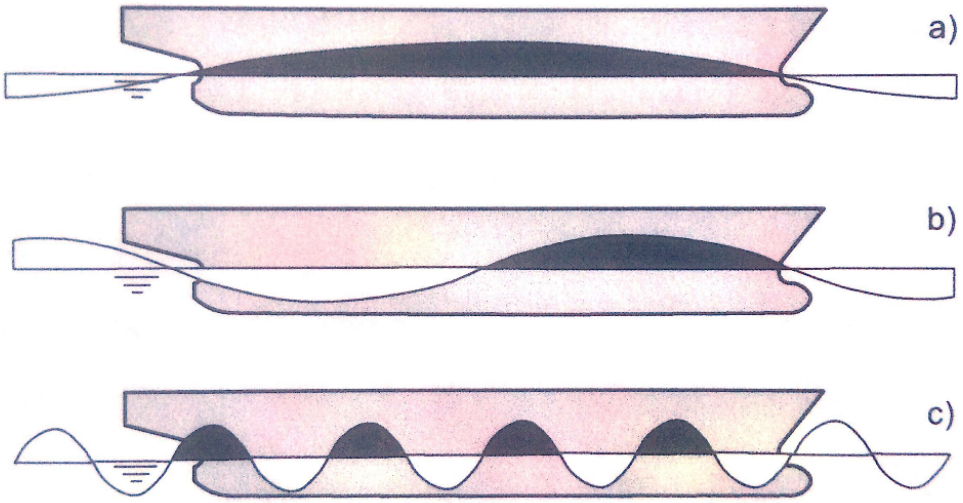

Figure 49: An indication of the wavelength to ship length ratio, λ/L. *a)* $\lambda = 2L$. *b)* $\lambda = L$. *c)* $\lambda << L$.*[1]*

this case, the ship length $L = 84.3m$, and the critical wave has the ratio of wavelength to ship length $\lambda/L = 1.04$.

Wave steepness

In Figure 43 and Figure 47, the dynamic VBM and VSF are indicated respectively. Among the curves plotted in the two figures, there are two sets of curves plotted with wide line type. One indicates the result of wave parameter $H_z = 8.5m$, $\lambda = 88m$, $H_z/\lambda = 1/10.4$, while the other one has the wave parameter $H_z = 7.5m$, $\lambda = 88m$, $H_z/\lambda = 1/11.7$. It can be seen, for the wave with larger wave steepness, both the dynamic VBM and VSF are more critical than the one whose steepness is smaller.

To judge the 1/7 limit, Table 7 is converted in terms of the steepness according to Table 3 as shown in Table 12. The steepness ranges from 1/10 to 1/282. None of the waves has steepness higher than 1/7. It can be seen that longer wave is albe to have larger steepness. It gives the inspiration that 1/7 could appear if the wavelength is larger, and even more steep waves could exist. However, those waves will impact on a ship when the ship length is close to the wavelength. Those ship do not exist yet. Nowadays, the limiatation of 1/7 for wave steepness is surficient in ship design.

4.3.2 Ship parameter

The ship parameters are very crucial, but in this thesis project, *Napastar* is the only model to be taken into use. No comparisons can be made. Fortunately, some clue can be found in the requirement from DNV-GL rule and IACS rule. As indicated in Equ. 45 and Equ. 46, the nonlinearity effect of the vertical bending moment and shear force relate close with the block coefficient C_B. The less C_B is, more effect of nonlinearity is discovered. Thus, all the parameters relating to C_B would impact the effect nonlinearity. For instance, large flare angle in strips makes C_B smaller

Table 12: Scatter static chart of waves in North Atlantic Sea in terms of wave steepness.

$H_z[m]$											
14.5											
13.5											
12.5											
11.5								1/15			
10.5							1/13	1/16	1/20		
9.5						1/12	1/15	1/18	1/22	1/26	
8.5					1/10	1/13	1/17	1/20	1/24	1/29	
7.5					1/12	1/15	1/19	1/23	1/28	1/33	
6.5				1/10	1/14	1/17	1/22	1/27	1/32	1/38	1/44
5.5				1/12	1/16	1/21	1/26	1/31	1/38	1/44	1/52
4.5				1/15	1/20	1/25	1/31	1/38	1/46	1/54	
3.5			1/14	1/19	1/25	1/32	1/40	1/49	1/59	1/70	
2.5			1/19	1/26	1/35	1/45	1/56	1/69	1/83	1/98	
1.5			1/32	1/44	1/59	1/75	1/94	1/115	1/138		
0.5		1/63	1/95	1/132	1/176	1/226	1/282				
$T_z[s]$	3.5	4.5	5.5	6.5	7.5	8.5	9.5	10.5	11.5	12.5	13.5

and leads to heavy effect of nonlinearity. Impact of the other parameters are to be studied in the future work.

4.4 Remarks for future development

Due to the time limitation, there are still some topics worth studying but left to do in the future development. One potential topic is to apply more other models, so that comparisons could be made and the influence from ship parameters can be studied. This could be useful in designing the ship hull in the very early stage. Also, *Napa* is one commercial software applicable for the calculation, and there are other softwares as well. Results derived by different softwares can be compared and the validation can be commented. Just like the saying "A workman must sharpen his tools if he is to do his work well", the motivation to select reliable design tool is crucial.

Another topic could be the application of *panel method*. In the progress of this thesis work, the *panel method* has been tried to apply, but errors happened. Since *Napa* company indicates the attitude to evaluate this module in 2016, it would be possbile to predict the hull girder loads during early design stage with *panel method* in the future. The accuracy and time-consumption could be a target to aim at.

For the ship design process, the further probability prediciton can be studied in the future work. With the wave spectrum, the transfer function and the response function of vertical bending moment, the probability that the ship would fail when

sailing in the sea state can be predicted. This prediction shall be combined with other critical aspects and the ship operability can be derived. Besides, methods shall be suggested to avoid accident that wave loads are large enough to damage the ship.

In this thesis, a general cargo ship model is used for the calculation. Seen from Figure 35, there are also many other seaborne ship types. The DNV-GL rule and IACS rule have extra rules for other ship types. For example, the tortional strength requirement is indicated in the rules for container ships. Studies against the tortional strength requirement can be studied in the future.

As mentioned, this thesis work is done for the educational purpose. To introduce the study process of the thesis in future education is also an aspect to work on.

5 Conclusion

In the thesis work, the ship response in vertical bending moment is calculated based on the statistic chart and the transfer function generated with *Napa*. The vertical bending moment and shear force along the ship is illustrated with respect to the critical waves determined according to the ship response calculation. The target of the thesis is to suggest a practical way to estimate the ship hull girder loads in early design stage. To achieve that, the problem is narrowed into the following two questions:

- How valid the DNV-GL rule and IACS rule are in requiring wave vertical bending moment and shear force along the ship?
- How feasible *Napa* is in checking the loads on ship hull girder during early design stage?

The validation of the DNV-GL rule and IACS rule in vertical bending moment and shear force has been discussed. The static and dynamic loads are ruled by DNV-GL and IACS. As discussed in the last section, there could be overestimaiton in static loads requirement from the ship class societies. The wave loads are not required by rules, but the results show an underestimation in wave loads calculated according to rules. The dynamic loads requirement, as the combination of static loads and wave loads, is quite reasonable.

The effect of nonlinearity has also been discussed. Both DNV-GL rule and IACS rule take it into consideration. The rules relate the effect of nonlinearity with the block coefficient C_B. The trend of the rule requirement matches that of the calculated vertical bending moment and shear force along the ship. Overall, the rules are judged valid.

The feasibility of *Napa* is discussed based on the accuracy and time consumption to go through the entire calculation process with *strip method* in *Napa*. It can be judged that the accuracy is quite acceptable for the early design stage, and the method is quite time saving. It is effecient to apply *Napa* to derive the hull girder loads. Thus, *Napa* is judged feasible for hull girder loads calculation.

Besides, the factors influencing the hull girder loads have been discussed. For wave parameters, the ratio of wavelength to ship length λ/L and the wave steepness H/λ are most important factors. The most critical wave appears as soon as the wavelength is close to ship length and the wave steepness is to be the highest. For the ship parameter, not many comments can be given, but those affecting block coefficient C_B could be crucial in the effect of nonlinearity. More study and research are expected to be done in the future development.

References

[1] Anders Rosén. *Naval Architecture Marine Dynamics.* KTH Centre for Naval Architecture 2015.

[2] *Naval-architecture* http://naval-architecture.blogspot.fi/ 24.5.2016.

[3] *UPDATE on MOL Comfort's Accident: PHOTOS* https://www.vesselfinder.com/news/1222-UPDATE-on-MOL-Comforts-Accident-PHOTOS 24.5.2016.

[4] Temarel, P., Chen, X.B., et. Al. 17th International Ship and Offshore Structures Congress 16-21 *Loads,* vol. 1, Committee I.2, s. Seoul, Korea, August 2009.

[5] *ROUGH SEAS' SAFE HANDS* http://www.safehavenmarineold.com/DAG%20PIKE%20article%20rough%20seas%20safe%20hands.htm 24.5.2016.

[6] Singh, S.P., Sen, D. *A comparative study on 3D wave load and pressure computations for different level of nonlinearities.* Marine Structures 2007;20, 1-24.

[7] Matusiak J. *Ship Dynamics.* Aalto University.

[8] Korvin Kroukovsky BV. *Investigation of Ship Motions in Regular Waves.* SNAME Trans 1955; 63.

[9] Korvin Kroukovsky, BV., Jacobs, WR. *Pitching and Heaving Motions of a Ship in Regular Waves.* SNAME Trans 1957;65:590-632.

[10] Jacobs, WR. *The Analytical Calculation of Ship Bending Moments in Regular Waves.* J Ship Res 1958; 2(2): 20-9.

[11] Salvesen, N., Tuck, E.O. *Ship Motions and Sea Loads.* SNAME Trans 1970;78:250-87.

[12] Tasai, F., Takagi, M. *Theory and Calculation of Ship Responses in Regular Waves.* Symposium on Seaworthiness, Society of naval Architects of Japan, 1969. p. 1-33.

[13] Borodai, IK., Netsvetayev, YA. *Ship Motions in Ocean Waves.* Leningrad: Studostorenie, 1969.

[14] Bishop, RED., Price, WG., Tam, PKY. *A Unified Dynamic Analysis of Ship Response to Waves.* RINA Trans 1977;119;363-90.

[15] Bishop, RED., Price, WG., Tam, PKY. *A Unified Dynamic Analysis of Antisymmetric Ship Response to Waves.* RINA Trans 1980;112:349-65.

[16] Gerritsma, J., Beukelman, W. *The Distribution of Hydrodynamic Forces on a Heaving and Pitching Ship Model in Still Water.* 5th Symposium on Naval Hydrodynamics. Washington D.C.: National Academy Press, 1964: 219-51.

[17] Wahab, R., Vink, JH. *The Hydrodynamic Forces and Ship Motions in Oblique Waves.* Netherlands Research Center TNO Report 193S, 1973.

[18] Newman, J.N. *he theory of ship motions [J].* Advances in applied mechanics,1978, 18: 221-285P.

[19] Wu, Y.S., Xia, J.Z., Du S.X. *Two Engineering Approaches to Hydroelastic Analysis of Slender Ships [J].* Dynamics of Marine Structure, 1991, 6(23): 143-163P.

[20] Faltinsen, O., Zhao, R. *Numerical predictions of ship motions at high forward speed.* Philos Trans R Soc London, Ser A 1991;334:241-52.

[21] Hermundstad, OA., Aarsn, SJV., Moan, T. *Linear Hydroelastic Analysis of High-speed Catamarans and Monohulls [J].* Journal of Ship Research, 1999,43 (1): 48-63P.

[22] Wu, MK., Moan, T. *Linear and Nonlinear Hydroelastic Analysis of High-speed Vessels.* J Ship Res 1996;40(2):149-63.

[23] Journée, J.M.J., and Adegeest, L.J.M. *Theoretical Manual of Strip Theory Program "SEAWAY for Windows".* TU Delft Report 1370 (2003).

[24] Jensen, JJ., Pedersen, PT. *Wave-induced Bending Moments in Ships – a Quadratic Theory.* RINA Trans 1979;121:151-65.

[25] Yamamoto, Y., Fujino, M., Fukasawa T. *Motion and Longitudinal Strength of a Ship in Head Sea and Effects of Nonlinearities.* J Soc Naval Architects Japan 1978;143:179-87, 1978;144:214-18, 1979;145:63-70.

[26] Meyerhoff, WK., Schlachter, G. *An Approach for the Determination of Hull Girder Loads in a Seaway including Hydro Dynamic Impacts.* Ocean Engng 1980; 7: 305-26.

[27] Fujino, M., Yoon, BS. *A Study on Loads Acting on a Ship in Large Amplitude Waves.* Naval Architecture and Ocean Engineering, J. Soc Naval Architects of Japan, 1986; 24: 39-57.

[28] Soares, CG. *Transient Response of Ship Hulls to Wave Impact.* Naval Int shipldg Prog. 1989; 36: 137-92.

[29] Xia, J., Gu M., Wu Y. *Time simulation of nonlinear hydroelastic response on ships[J].* Selected Paper of Chinese Society of Naval Architecture and Marine Engineering, 1988, 3: 125-134P.

[30] Söding, H. *Leckstabilitat in Seegang.* Report 429 of the Institute fur Schiffbau Humburg, 1982.

[31] Bottcher, H. *Simulation of Ship Motions in a Seaway.* Report 498 of the Institute fur Schiffbau der Universitat Hamberg, 1989.

[32] Schlachter, G. *Hull Girder Loads in a Seaway Including Non-linear Effects [J].* Schiffstechnic, 1989,36:169-180P.

[33] Xia, J., Wang Z. *Time-domain hydroelasticity theory of ships responding to waves [J].* J Ship Res 1997;41(4):286-300.

[34] Jensen, J.J., Dogliani M. *Wave-induced Ship Hull Vibrations in Stochoastic Sea Ways.* Marine Structures, 1996, 9(3): 353-387P.

[35] Xia, J., Wang Z., Jensen J.J. *Non-linear Wave Loads and Ship Responses by a Time Domain Strip Theory.* Marine Structures, 1998, 11(3):101-123P.

[36] Watanabe, I., Guedes Soares C. *Comparative Study on the Time-domain Analysis of Non-linear Ship Motions and Loads.* Marine Structures 12.3 (1999): 153-170.

[37] Tao, Z., Incecik A. *Non-linear Motions and Global Bending Moments in Regular Head Seas.* In: Murthy TKS., Wilson PA., Wadhams P., editors. Marine offshore and ice technology. Southampton: Computational Mechanics Publications, 1994.

[38] Fonseca, N., Guedes Soares C. *Time-domain Simulation of Vertical Ship Motions.* In: Murthy TKS., Wilson PA., Wadhams P., editors. Marine offshore and ice technology. Southampton: Computational Mechanics Publications, 1994. p. 224-43.

[39] Fonseca, N., Guedes Soares C. *Time-domain Analysis of Large-amplitude Vertical Motions and Wave Loads.* J Ship Res. 1998;42(2):100-13.

[40] Ramos, J., Guedes Soares C. *Vibratory Response of Ship Hulls to Wave Impact Loads.* Int Shipbuilding Prog 1998;45(441):71-8.

[41] Kring, DC., Huang YF., Sclavonous PD., Vada T., Braathen A. *Non-linear Ship Motions and Wave-induced Loads by a Rankine Panel Method.* Proceedings of 21st Symposium on Naval Hydrodyn, Trondheim, 1996. p. 16-33.

[42] Xia, J., Wang Z., Gu X., Shen J., Wu Y. *Numerical Simulation of the Wave-induced Non-linear Bending Moment of Ships.* Proceedings of the 14th Conference on Offshore Mechanics and Arctic Engineering, 1995. vol. II. pp. 147-53.

[43] Yamamoto, Y., Fujino M., Fukasawa T., Ohtsubo H. *Slamming and Whipping of Ships Among Rough Seas.* Numerical analysis of the dynamics of ship structures. Proceedings of EUROMECH Colloquium 122, Paris, 1979, p. 19-33.

[44] Watanabe, I., Sawada H. *Effects of Elastic Responses to the Longitudinal Bending Moment in Two- directional Waves.* Naval Architecture Mar Eng, 1986;24:91-102.

[45] Hess, J.L., Smith A.M.O. *Calculation of Non-lifting Potential Flow about Arbitrary Three-dimensional Bodies.* Journal of Ship Research, 1964, 8(2):22-44P

[46] Wu, Y.S. *Hydroelasticity of Floating Bodies [D].* Brunel University, U. K., 1984

[47] Price, W.G., Wu Y.S. *Hydroelasticity of marine structures [J].* Theoretical and Applied Mechanics, 1985: 311-337P

[48] Bishop, R.E.D., Price W.G., Wu, Y. *A General Linear Hydroelasticity Theory of Floating Structures Moving in a Seaway.* Philosophical Transactions of Royal Society, 1986, London, A316.

[49] Aksu, S., Price W.G., Suhrbier, K.R. *A Comparative Study of the Dynamic Behavior of Fast Patrol Boat Traveling in Rough Sea [J].* Marine Structure, 1993, 6(5 6): 421-411P

[50] Du, S.X. *A Complete Frequency Domain Analysis Method of Linear Three-dimensional Hydroelastic Responses of Floating Structure Travelling in Waves.* PhD. Thesis, China Ship Scientific Research Center, Wuxi, China, 1996.

[51] Lundgren, J., Price W.G., Wu, Y.S., *A Hydroelastic Investigation into the Behavior of a Floating 'dry' Dock in Waves.* Spring Meeting of Royal Institution of Naval Architects, London 1988.

[52] Wu, Y.S., Maeda H., Kinoshita, T., *The Second Order Hydrodynamic Actions on a Flexible Body.* Tokyo, 1997.

[53] Tian, C., Wu Y.S. *The Second-order Hydroelastic Analysis of a SWATH Ship Moving in Large-amplitude Waves [J].* Hydrodynamics, Ser. B., 2006, 18(6): 631-639P.

[54] Gadd, G.E. *A Method of Computing the Flow and Surface Wave Pattern around Full Forms.* Trans, Roy, Asst. Nav. Archit., Vol. 113. 1976.

[55] Dawson, C.W. *A Practical Computer Method for Solving Ship-wave Problems.* 2nd International Conference on Numerical Ship Hydro dynamics, USA, 1977.

[56] *NAPA for Design 2015.4 Manuals.*

[57] *Presentation on theme: "Ship is so far assumed to be in calm water to determine."* http://slideplayer.com/slide/4213394/ 25.5.2016

[58] *WIKIPEDIA* https://en.wikipedia.org/wiki/Fourier_transform 10.5.2016

[59] Yoshida T., Chang-Kyu R. *SAR Image Simulation in the Time Domain for Moving Ocean Surfaces.* Sensors 13.4 (2013): 4450-4467.

[60] Faltinsen O. *Sea Loads on Ships and Offshore Structures.* Vol. 1. Cambridge university press, 1993.

[61] *WIKIPEDIA* https://en.wikipedia.org/wiki/Stokes_wave 11.5.2016

[62] Huss M. *Vågor och Gensvar.* KTH, Department of Naval Architecture, 1983.

[63] *Wave Data Analysis and Statistics* http://new.mhl.nsw.gov.au/data/realtime/wave/AnalysisAndStatistics 25.5.2016.

[64] Hogben N., Dacunha NMC., Olliver GF. *Global Wave Statistics.* London: Unwin Brothers, 1986.

[65] Michel K. Ochi. *Marine Environments and Its Impact on the Design of Ships and Marine Structures.* Centennial Meeting of the Society of Naval Architects and Marine Engineers, September 1993.

[66] Bretschneider C.L. *Wave Variability and Wave Spectra for Wind-generated Gravity Waves.* No. TM-118. CORPS OF ENGINEERS WASHINGTON DC BEACH EROSION BOARD, 1959.

[67] DNV-GL *Rules for classification: Ships.* Edition October 2015, amended January 2016.

[68] *WIKIPEDIA* https://en.wikipedia.org/wiki/Hogging_and_sagging 19.5.2016.

[69] IACS *Definition of Ship's Length L and of Block Coefficient C_b.* S2, Rev.1 May 2010.

[70] IACS *Longitudinal Strength Standard.* S11, Rev.6 May 2010.

[71] Kendrick, A., Daley C., Pavic. M. *Comparative Study of Ship Structure Design Standards.* Ship Structures Committee Report SR-1444, submitted to US Maritime Administration, by BMT Fleet Technology (2006).

[72] Akira Nitta, Hironori Arai, and Atsushi Magaino. *Basis of IACS Unified Longitudinal Strength Standard.* Marine Structures 5.1 (1992): 1-21.

[73] Hideomi Ohtsubo, and Takao Kuroiwa. *Non-linearity in Sagging Moment and Shear Force of Fine Ships.* Technical Bulletin of Nippon Kaiji Kyokai 7 (1989): 1-10.

A Drawings and ship parameters

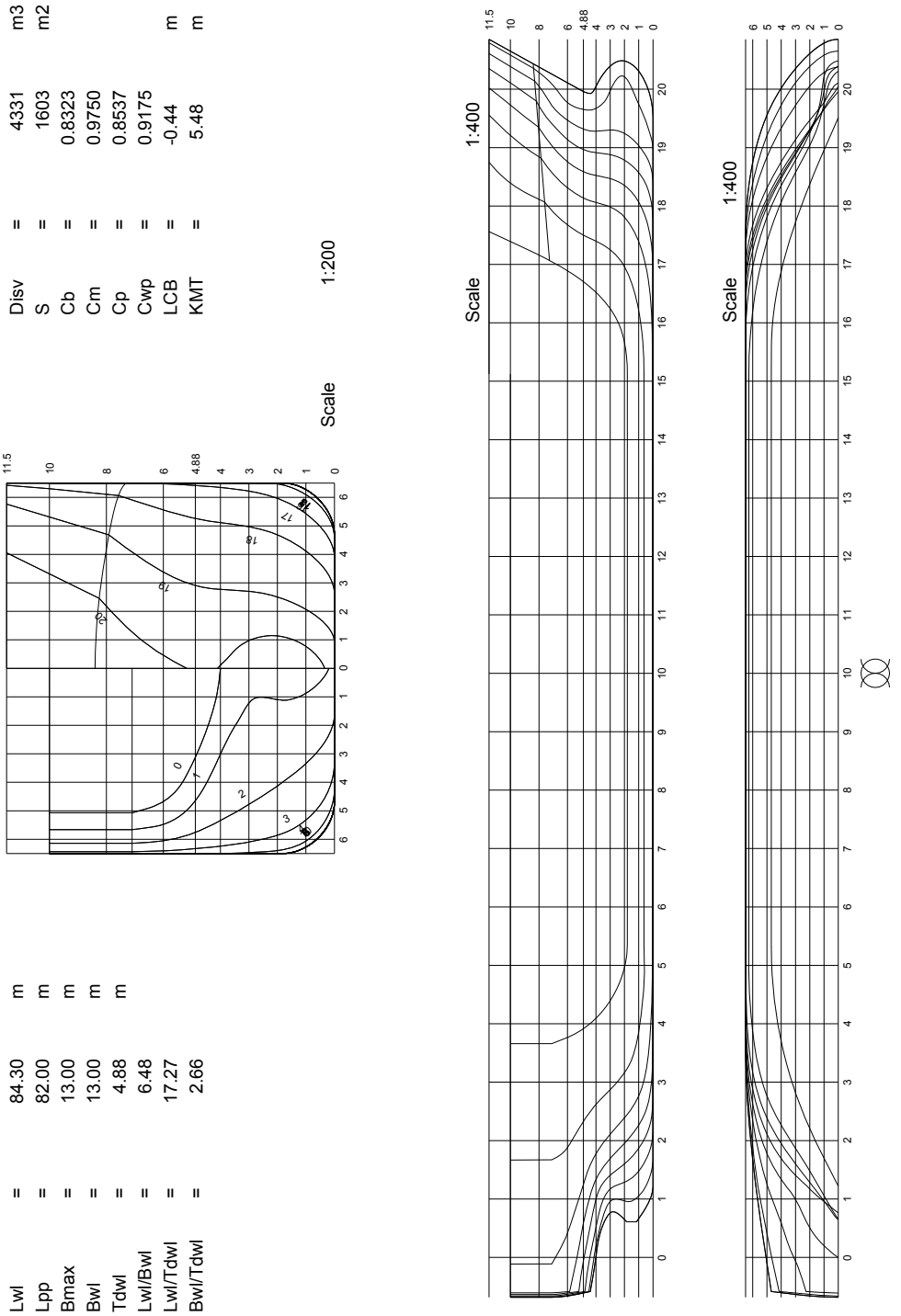

Figure A1: Ship hull drawings and main parameters

B Full loading condition

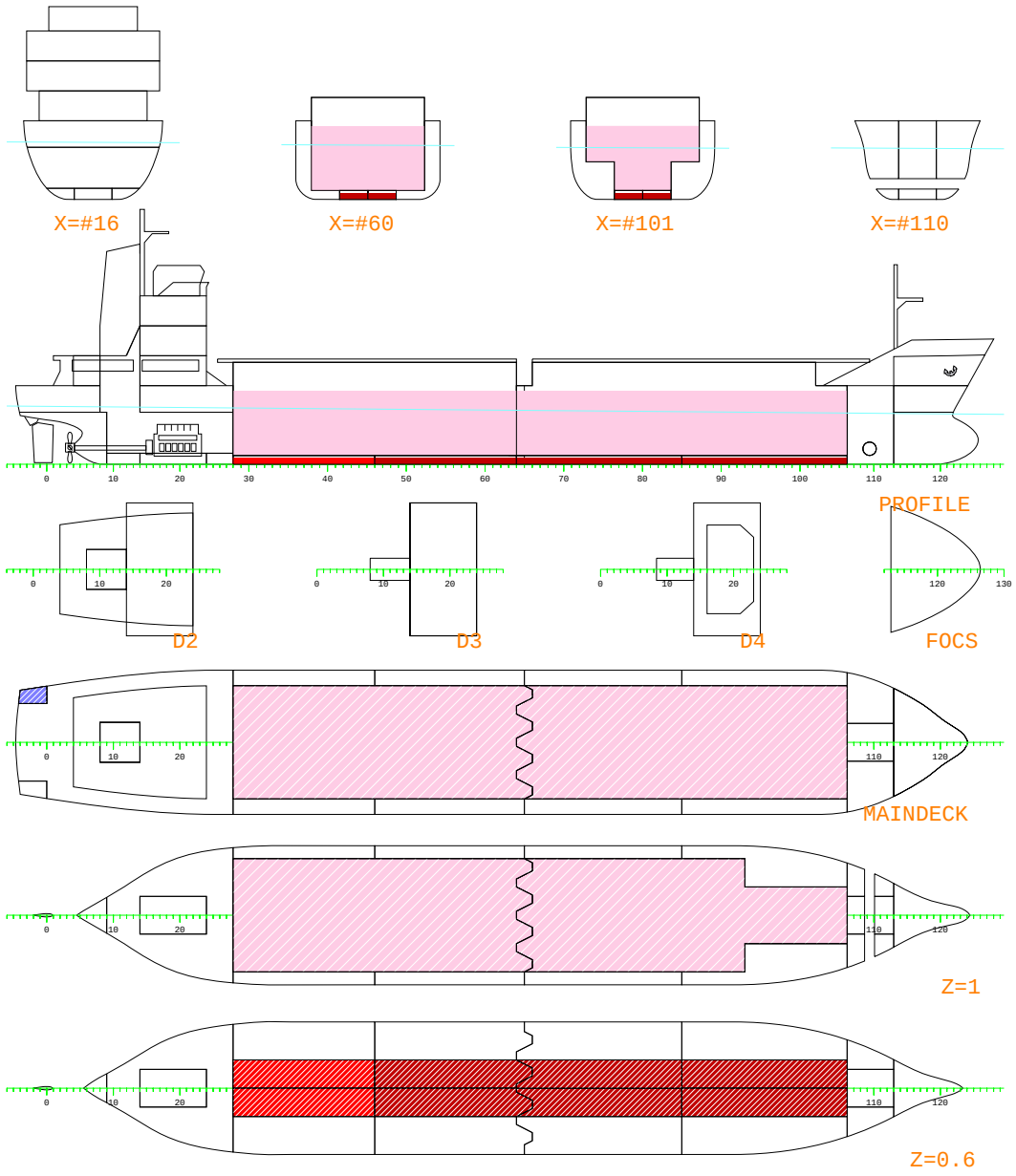

Figure B1: An indication of full loading condition

Table B1: The tank filling condition in ship full loading condition

Name	Max. weight	Mass	Center of gravity cgx	cgy	cgz	Free s. moment
Cargo, RHO=1.000						
R03011 HOLD1	2244.7	1571.3	56.90	0.00	3.84	2503.32
R02011 HOLD2	2195.5	1536.9	29.98	0.00	3.72	2296.20
Total of CA	4440.3	3108.2	43.59	0.00	3.78	4799.52
Diesel oil, RHO=0.860						
R02001 DBtank 6 PS .	20.9	14.6	23.19	1.28	0.27	0.00
R02002 DBtank 6 SB .	20.9	14.6	23.19	-1.28	0.27	0.00
Total of DO	41.7	29.2	23.19	0.00	0.27	0.00
Fresh water, RHO=1.000						
R00021 Fresh Water	3.9	2.7	-1.08	3.99	6.13	0.00
Heavy Fuel Oil, RHO=0.940						
R03002 DBtank 4 SB .	25.2	17.6	50.21	-1.26	0.27	0.00
R02005 DBtank 6 PS .	24.3	17.0	36.39	1.29	0.27	0.00
R02006 DBtank 5 SB .	24.3	17.0	36.39	-1.29	0.27	0.00
R03005 DBtank 3 PS .	26.6	18.6	64.73	1.28	0.27	0.00
R03006 DBtank 3 SB .	26.6	18.6	64.73	-1.28	0.27	0.00
R03001 DBtank 4 PS .	25.2	17.6	50.21	1.26	0.27	0.00
Total of HFO	152.1	106.5	50.88	0.00	0.27	0.00
Miscellaneous, RHO=1.000						
R01001 Miscellaneous	67.2	0.0	12.45	0.00	0.54	583.48
Deadweight		3246.6	43.61	0.00	3.63	5383.0
Lightweight		1200.0	32.00	0.00	4.20	
Displacement (rho=1.025)		4446.6	40.47	0.00	3.79	5383.0

F L O A T I N G P O S I T I O N

Draught moulded	4.881	m	KM	5.49 m
Trim	-0.689	m	KG	3.79 m
Heel, PS=+	0.3	deg		
TA	5.226	m	GM0	1.70 m
TF	4.537	m	GMCORR	-1.21 m
Trimming moment	-4182	tonm	GM	0.49 m

LOADING CONDITION LOAD3, Departure Condition

Table B2: Ship parameters in full loading floating position

```
2 General Information
2.1 Ship Information
2.1.1 Main Dimension
Calculation method : Strip method
Parameters calculated according to given floating position
and actual geometry of surface HULL


T         Draught, mean                  4.881      m
Ta        Draught aft                    5.226      m
Tf        Draught fore                   4.537      m
Lpp       Length between perpend.        82.00      m
wl lengthlength of waterline             84.30      m
LCB       long. centre of buoy.         -0.442      m
Disv      Moulded disp. volume            4283     m3
Bwl       Breadth of waterline           13.00      m
Lwl/Bwl   Length/Beam ratio              6.484
Bwl/T     Breadth/draught ratio           2.66
Lwl/T     Length to Draught ratio        17.27
Lwl/Disv  Length to Vol ratio            5.172
S         Wetted surface area             1603     m2
SVr       S/Disv^(2/3)                   6.032
CVol      Disv/Lwl^3                     7.230    E-3
CS        S coeff. S/SQRT(Disv*Lpp)      2.653
CAbt      Abt / Ax                         9.7      %
CAtr      Atrans / Ax                      0.0      %
BVr       Beam/Disv^(1/3)                0.798
TVr       T/Disv^(1/3)                   0.299
Enta      Half angle of entrance         35.68    deg
CB        block coefficient             0.8323
CM        midship section coeff.         0.975
Cp        prismatic coefficient         0.8537
GM        Initial GM                      0.49      m
KMT       transv. metac. height          5.476      m
VCG       Vertical height of CG           4.99      m
LCB       % of LWL                        48.11      %
LCB       % of LPP                        49.46      %
2.1.2 Radius of Gyration
Loading Condition used for Radius of Gyration Calculation : LOAD3

KXX   Roll  radius of gyration / B  0.2595
KYY   Pitch radius of gyration / L  0.1961
KZZ   Yaw   radius of gyration / L  0.1980
KXY   Cross radius of gyration / L  0.0047
KXZ   Cross radius of gyration / L  0.0099
KYZ   Cross radius of gyration / L  0.0011
```

C Strip division and regular wave defination

Table C1: Strip defination

2.2.2 Sectional Area
Hull sections to be used in the strip calculations:

Frxcor	Frx m	Frbwli	Frti	Frarea	Frccg	Frycg
-1.0140	-0.575	0.5568	0.2353	0.0799	0.0890	0.1001
-0.9161	3.439	0.7381	0.9563	0.2331	0.2579	0.1140
-0.8182	7.453	0.8810	1.0577	0.6491	0.4425	0.1658
-0.7203	11.468	0.9655	1.0508	0.9016	0.4917	0.2178
-0.6224	15.482	0.9995	1.0439	0.9930	0.5044	0.2393
-0.5245	19.496	1.0000	1.0370	1.0111	0.5076	0.2447
-0.4266	23.510	1.0000	1.0301	1.0059	0.5047	0.2447
-0.3287	27.524	1.0000	1.0232	0.9989	0.5013	0.2447
-0.2308	31.539	1.0000	1.0163	0.9920	0.4978	0.2447
-0.1329	35.553	1.0000	1.0094	0.9851	0.4944	0.2446
-0.0350	39.567	1.0000	1.0025	0.9782	0.4910	0.2446
0.0630	43.581	1.0000	0.9956	0.9713	0.4875	0.2445
0.1609	47.595	1.0000	0.9886	0.9644	0.4841	0.2445
0.2588	51.609	1.0000	0.9817	0.9575	0.4806	0.2445
0.3567	55.624	1.0000	0.9748	0.9506	0.4772	0.2444
0.4546	59.638	1.0000	0.9679	0.9437	0.4738	0.2444
0.5525	63.652	1.0000	0.9610	0.9364	0.4697	0.2440
0.6504	67.666	1.0000	0.9541	0.9019	0.4583	0.2375
0.7483	71.680	0.9211	0.9472	0.7779	0.4449	0.2081
0.8462	75.695	0.6527	0.9403	0.5164	0.4304	0.1434
0.9441	79.709	0.2427	0.9334	0.2111	0.4271	0.0589

Table C2: Wave defination

2.3 Calculation Parameters
2.3.1 Heading angle

Heading deg
0.00
45.00
90.00
135.00
180.00

2.3.2 Ship speed

Vs knots	Fn
0.000	0.000
15.000	0.268

2.3.3 Inputs for Regular Wave Analysis

SqrLPLa	WLen m	LPLA	LaLp	WPer sec	Omega 1/s	Hz 1/s
0.1500	3644.4	0.023	44.444	48.314	0.1300	0.0207
0.2000	2050.0	0.040	25.000	36.235	0.1734	0.0276
0.2500	1312.0	0.062	16.000	28.988	0.2167	0.0345
0.3000	911.1	0.090	11.111	24.157	0.2601	0.0414
0.4000	512.5	0.160	6.250	18.118	0.3468	0.0552
0.4500	404.9	0.202	4.938	16.105	0.3901	0.0621
0.5000	328.0	0.250	4.000	14.494	0.4335	0.0690
0.5500	271.1	0.303	3.306	13.176	0.4768	0.0759
0.6000	227.8	0.360	2.778	12.078	0.5202	0.0828
0.6500	194.1	0.422	2.367	11.149	0.5635	0.0897
0.7000	167.3	0.490	2.041	10.353	0.6069	0.0966
0.8000	128.1	0.640	1.562	9.059	0.6936	0.1104
0.9000	101.2	0.810	1.235	8.052	0.7803	0.1242
1.0000	82.0	1.000	1.000	7.247	0.8670	0.1380
1.1000	67.8	1.210	0.826	6.588	0.9537	0.1518
1.2000	56.9	1.440	0.694	6.039	1.0404	0.1656
1.3000	48.5	1.690	0.592	5.575	1.1271	0.1794
1.5000	36.4	2.250	0.444	4.831	1.3005	0.2070
1.8000	25.3	3.240	0.309	4.026	1.5606	0.2484
2.2000	16.9	4.840	0.207	3.294	1.9074	0.3036
2.7000	11.2	7.290	0.137	2.684	2.3409	0.3726
5.5000	2.7	30.250	0.033	1.318	4.7685	0.7589